UG
A32A11
1968
6

TS

OAR RESEARCH REVIEW

OFFICE OF AEROSPACE RESEARCH ★ UNITED STATES AIR FORCE

OAR: The Research Agency of the United States Air Force

Volume VIII Number 6 November-December 1969

OAR RESEARCH REVIEW

VOLUME VIII NUMBER 6 Nov-Dec 1969

POWERFUL NEW SOLAR TELESCOPE BECOMES OPERATIONAL	2	Sacramento Peak Observatory, AFCRL
PREFERENTIAL DISSOLUTION IN Fe-Ni ALLOYS	3	Lt Dale O. Condit, Metallurgy and Ceramics Research Laboratory, ARL
METALLURGICAL STUDIES OF HIGH-RATE DEFORMATION	5	Drs. J. D. Boyd, G. T. Hahn and A. R. Rosenfield, Metal Science Group, Battelle Memorial Institute, Columbus, Ohio
WATER IN A VACUUM AND LUNAR RIVERS	7	Space Physics Laboratory, AFCRL
BUCKLING AND POSTBUCKLING OF OVAL CYLINDRICAL SHELL UNDER AXIAL COMPRESSION	9	Dr. Joseph Kempner, Polytechnic Institute of Brooklyn, New York
LOW-FREQUENCY AIRCRAFT COMMUNICATIONS SYSTEM	13	Ionospheric Physics Laboratory, AFCRL
THE HYPERSONIC ROLL-DAMPING DERIVATIVE OF A BLUNT CONE	14	Dr. Brian Quinn, Energetics Research Laboratory, ARL
ON HEATING AN ELECTRON	16	La Verne E. Woods, Research Information Office, AFCRL
MAGNETIC FREEZE-OUT: THE ROLE OF IMPURITY DENSITY FLUCTUATIONS	18	Dr. L. J. Neuringer, Francis Bitter National Magnet Laboratory, MIT
AEROELASTIC STABILITY OF THIN CYLINDRICAL SHELLS	20	Dr. Jacob Pomerantz, Directorate of Engineering Sciences, AFOSR
PROOF OF A PERFECT CODE	22	Data Sciences Laboratory, AFCRL
TRANSDUCER-SENSOR GENERATION GAP	23	Capt John F. Kantak, Directorate of Engineering Sciences, AFOSR

CLOUD PATTERNS ON A SUMMER DAY	28	Meteorology Laboratory, AFCRL
ARGON PLASMA SPECTROSCOPY	30	Dr. W. G. Braun, Plasma Physics Research Laboratory, ARL
SOME RECENT DEVELOPMENTS IN STRONG INTERACTION PHYSICS	32	Dr. Erich Weigold, Directorate of Physical Sciences, AFOSR
PERCEPTION VS. IMAGERY	34	Dr. Glen Finch, Directorate of Life Sciences, AFOSR
A LITTLE BIT OF DATA	35	Lt Col Robert B. Kalisch, Directorate of Engineering Sciences, AFOSR
IMPROVING THE QUALITY OF WEATHER-SATELLITE PHOTOS	36	Meteorology Laboratory, AFCRL
NEW RADAR TECHNIQUE FOR DETECTING CLOUDY-AIR TURBULENCE	37	Meteorology Laboratory, AFCRL

ON THE COVER:

AFCRL's new vacuum tower telescope, which took three years to build, became operational in October 1969. With a total length of 365 feet (227 feet of which are beneath ground level), it will give the Air Force observatory at Sacramento Peak, N.M. a unique instrument for observing features on the sun. (See article in this issue, "Powerful New Solar Telescope Becomes Operational.")

OAR RESEARCH REVIEW is published bimonthly by the Office of Scientific and Technical Information (RRYC), Hq Office of Aerospace Research, USAF, 1400 Wilson Boulevard, Arlington, Va. 22209. The objective of this publication is to make a positive contribution to the exchange of information concerning Air Force conducted and sponsored research activities.

JACOB SEIDEN *Editor*

For sale by the Superintendent of Documents, U.S. Government Printing Office, Washington, D.C. 20402 – $3.00 per year domestic, 75 cents additional for foreign mailing, 45 cents per single copy and 30 cents per Annual Index. Back issues will not be furnished.

THIS DOCUMENT HAS BEEN APPROVED FOR PUBLIC RELEASE AND SALE; ITS DISTRIBUTION IS UNLIMITED.

powerful new solar telescope becomes operational

SACRAMENTO PEAK OBSERVATORY, AFCRL

AFCRL's vacuum tower telescope (see front cover), which became operational in October 1969, is the most important new solar observing instrument to be constructed anywhere in the world within the past decade. It is a unique instrument, the first in a new generation of specialized solar-observing instruments. With a resolving power of less than 0.2 sec of arc, the telescope's acuity matches that of the most powerful telescopes–stellar or solar–in the world. The addition of this telescope to those already in use at the Air Force's Sacramento Peak Observatory in southeast New Mexico makes the Observatory the most complete in the country for conducting solar astronomy.

The telescope is 365 feet long. Of this vertical length, 227 feet are set in a deep shaft beneath the ground. The above-ground portion of the telescope is enclosed in a massive conical tower 138 feet high. The central core of the telescope consists of a 321-foot long cylinder having a maximum diameter of 10 feet. The entire optics of the system–from the objective port at the top of the tower to the 64-inch reflecting mirror at the bottom of the shaft–is contained in this evacuated chamber. The telescope was based on a design conceived by Dr. Richard B. Dunn of Sacramento Peak Observatory. Construction of the $3.3 million tower telescope began in April 1966.

The combination of the tower and vacuum features in a telescope of the size and complexity of the new Sacramento Peak telescope will give astronomers at the Observatory an instrument of unequaled image stability. The objective port is located well above most of the air turbulence and heat currents that swirl up when the sun heats the ground. This eliminates a major source of image dancing and jitter which obscure detail. Further image stability is achieved by enclosing the optical system in a vacuum, thereby eliminating internal air currents. This central evacuated chamber weighs 250 tons and is evacuated to 250 torr, a pressure which corresponds to that found at an altitude of about 180,000 feet.

Additional protection against image-distorting heat currents is provided by embedding water-cooled pipes in the concrete walls of the tower. By controlling the temperature of the water flowing in these pipes, the temperature of the tower walls can be maintained at equilibrium with the air temperature inside the tower.

The evacuated central optical assembly rotates to follow the sun. The entire assembly is suspended from above like a pendulum and floats on an 11-ton pool of mercury located near the top of the tower. The mercury provides a friction-free bearing for the entire core assembly, which rotates at 1 revolution per minute.

The telescope itself has an aperture of 76 cm. Light from the sun enters through a quartz window 10 inches thick and 30 inches in diameter. Two flat mirrors, each 40 inches in diameter, reflect the light (first along a brief horizontal path, then downward) through the 321-foot length of the cylinder to a focusing mirror 183 feet beneath ground level. This 64-inch focusing mirror has a focal length of 180 feet. It can be tilted to direct light upward again and to form an image of the sun on one of several selected instruments at ground level.

All of the instruments are clustered about the central shaft and rotate with the shaft. The largest of these instruments are 3 evacuated spectrographs, each 68 feet long and 5 feet in diameter. These spectrographs are mounted vertically to the central core. Smaller instruments are located on the 40-foot-diameter rotating platform at ground level.

The vacuum telescope is an important adjunct to the nation's space program, particularly in the study of high-energy proton showers associated with sunspot activity. Such showers cause widespread radio blackout in the arctic and are hazardous to men in space.

Dr. Richard B. Dunn is a research physicist at AFCRL's Sacramento Peak Observatory, Sunspot, New Mexico. He conceived and designed the solar vacuum tower telescope at the Sacramento Peak Observatory.

Dr. Dunn received the B.S. in Mechanical Engineering (1949), and the M.S. in Astronomy (1950), both from the University of Minnesota. He also received a Ph.D. from Harvard in 1961.

From 1950-1953, Dr. Dunn was a teaching fellow and graduate student in astronomy at Harvard. He joined the staff of AFCRL's Sacramento Peak Observatory in 1953.

Dr. Dunn has gained an international reputation for the design and refinement of high-resolution solar telescopes and monochromatic filters. He has developed new photographic, photoelectric, and spectrographic techniques that have produced the highest-definition observations ever achieved of spicules, the fur-like filaments in the solar chromosphere.

Dr. Dunn is a member of the Solar Physics Panel of NASA's Astronomy Missions Board. He is also a member of Commission 10 of the International Astronomical Union, and of the American Astronomical Society.

Dr. Richard B. Dunn conceived the design for the solar vacuum tower telescope at the Sacramento Peak Observatory, and was the project scientist during its construction.

PREFERENTIAL DISSOLUTION IN Fe-Ni ALLOYS

LT DALE O. CONDIT
Metallurgy and Ceramics Research Laboratory, ARL

Stress corrosion cracking is one of the most serious materials problems in the Air Force today. It pervades the entire materials spectrum, from the stainless steels to aluminum airframes. One of the most recent theories concerning stress corrosion cracking in stainless steels depends for its validity on an initial enrichment step. During this step, atoms of the more active element(s) in an alloy dissolve preferentially, leaving behind an ennobled surface of the less active atomic species. In order to test this theory, one must determine the dissolution behavior of metals and alloys in a quantitative manner. Pickering (1, 2, 3) has used a very sensitive electrochemical technique to determine the dissolution behavior of Cu-Au and Cu-Zn alloys. However, this technique is not applicable because the equilibrium potentials of the components of the Fe-Cr-Ni system all lie below the H^+/H_2 equilibrium potential in acid solution.

This enrichment phenomenon has been demonstrated in Fe-Ni alloys in an investigation of the dissolution characteristics of alloys in this system. Five Fe-Ni binary alloys, pure Fe, and pure Ni were dissolved electrochemically in a 1N H_2SO_4 solution at various potentials in the active region of dissolution. At selected times during the potentiostatic dissolution, samples of the acid solution were removed from the test cell and analyzed, using an atomic absorption spectrometer to determine the concentrations of Fe and Ni present.

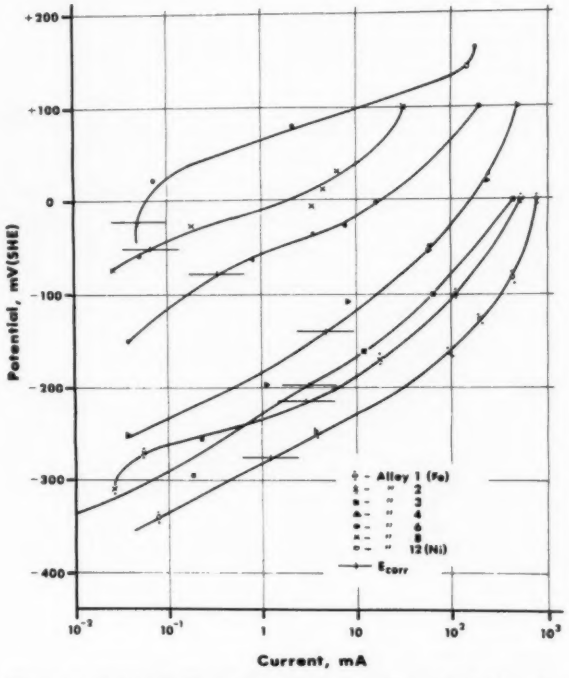

Figure 1. Total anodic polarization curves determined from the weight changes for the alloys investigated.

Using the specimen weight losses, the total anodic polarization curves were determined for each alloy. The calculations were checked using the concentrations of Fe and Ni in the solution and using the integrated current. These polarization curves, shown in Figure 1, indicated that the dissolution behavior of Fe-Ni alloys in the active region may be a structure sensitive property. The corrosion currents are an order of magnitude lower for alloys containing more than 20 atomic percent Ni than for those alloys containing less than 20 atomic percent Ni. This inflection in the corrosion behavior coincides with the change in structure in Fe-Ni alloys from body-centered cubic at low Ni concentrations to face-centered cubic at high Ni concentrations.

Electron metallographic studies also illustrated that Ni concentration in the alloy has an effect on the dissolution behavior, specifically at high dissolution potentials. The surface morphology for Fe-5Ni was characterized by ledges intersecting at angles of about 60°, whereas an Fe-20Ni alloy, with the same amount of surface dissolved, exhibited grooving or trenching of the surface rather than a geometric morphology. Dissolution rates for the same alloy also reduced the time required to form the ledges and grooves on the surface of the alloy.

Each Fe and Ni concentration was found to obey a dissolution rate law that:

$$C_i = a_i \, t^{n_i} \qquad (1)$$

where C_i is the concentration of Fe or Ni in solution in ppm, a_i is a constant, t is time, and n_i is the slope of the logarithmic equation. A computer solution for the method of least squares was used to determine the values of a_i and n_i for each alloy at each dissolution potential. These values are shown in Table I.

Equation (1) was also used to determine a zero-order intrinsic rate constant for Fe and Ni in an alloy. This rate constant was normalized by dividing each calculated rate constant by the respective concentration of Fe or Ni in the alloy. The rate constant was determined from the equation:

$$K_i = \frac{M_s}{A M_i N_i} \left(\frac{dc_i}{dt} \right) \times 10^{-6} \qquad (2)$$

where M_s is the mass of the solution in grams; A, the area of the specimen; M_i, the molecular weight of Fe or Ni; and N_i, the atomic percentage of Fe or Ni in the alloy. K_i is then given in moles/cm^2 · sec. Substituting equation (1), the intrinsic rate constant is given by:

$$K_i = K \, a_i \, n_i \, t^{(n_i - 1)} \qquad (3)$$

The value of n_i was approximately 1.0 for Fe, Fe in the alloys, and Ni in the alloys; and n_i was approximately 0.7 for pure Ni. As a first approximation, n_i was assumed to be 1.0 and the values for K_{Fe} and K_{Ni} were determined at three potentials of dissolution: -100m V, 0m V, and +100m V(SHE). The results of these calculations are shown in Figure 2. The shaded areas at each potential indicate where the rate of Fe dissolution exceeds the rate of Ni dissolution, i.e., where Ni enrichment could be expected to occur. The figure indicates that the probability for Ni enrichment increases with potential in the range of low Ni compositions.

The recent theory advanced for the mechanism of stress corrosion cracking is supported by the data obtained in this study. The results of this investigation also indicate that this enrichment process may be active in other systems. Studies have been undertaken to determine if this enrichment mechanism occurs in the Ti-Al alloy system.

Alloy	Potential mV (SHE)	n_{Fe}	n_{Ni}	$a_{\frac{Fe}{ppm}}$	$a_{\frac{Ni}{ppm}}$
Fe	0	1.02		1.01	
	-83	0.973		7.32×10^{-1}	
	-128	1.30		3.04×10^{-2}	
	-163	1.61		1.76×10^{-3}	
	-248	1.26		6.78×10^{-4}	
Fe- 5Ni	0	1.04	1.05	5.57×10^{-1}	2.89×10^{-2}
	-100	0.470	0.851	7.02	2.43×10^{-2}
	-170	1.09	0.905	1.32×10^{-2}	2.65×10^{-3}
Fe-10Ni	0	0.930	0.637	9.39×10^{-1}	3.30×10^{-1}
	-100	0.955	0.924	2.54×10^{-2}	1.83×10^{-2}
	-160	1.46	1.40	1.59×10^{-4}	9.85×10^{-5}
Fe-20Ni	+90	1.03	0.988	4.73×10^{-1}	1.55×10^{-1}
	+22	1.34	1.04	2.91×10^{-2}	5.15×10^{-2}
	-53	1.47	1.11	2.33×10^{-3}	7.30×10^{-3}
	-83	1.01	0.883	3.11×10^{-2}	2.81×10^{-2}
	-108	1.14	1.11	2.76×10^{-3}	1.11×10^{-3}
Fe-45Ni	+100	1.46	1.08	5.29×10^{-3}	6.37×10^{-2}
	+2	1.01	1.16	1.12×10^{-2}	3.04×10^{-3}
	-18	0.506	0.848	2.26×10^{-1}	1.48×10^{-2}
	-35	0.706	0.974	2.57×10^{-2}	2.79×10^{-3}
	-63	1.40	1.37	1.64×10^{-5}	2.43×10^{-5}
Fe-65Ni	+100	0.960	1.05	2.32×10^{-2}	1.91×10^{-2}
	+32	1.07	0.964	1.32×10^{-3}	7.77×10^{-3}
	+12	1.00	1.06	1.88×10^{-3}	2.61×10^{-3}
	-8	1.34	1.11	1.09×10^{-4}	1.44×10^{-3}
Ni	+162		0.690		2.52×10^{-1}
	+142		0.627		1.73×10^{-1}
	+90		0.803		1.38×10^{-2}
	+22		0.671		1.77×10^{-3}

TABLE 1

Values of n_i and a_i for the Rate-Law Equation for Fe and Ni in the Metals and Alloys Investigated

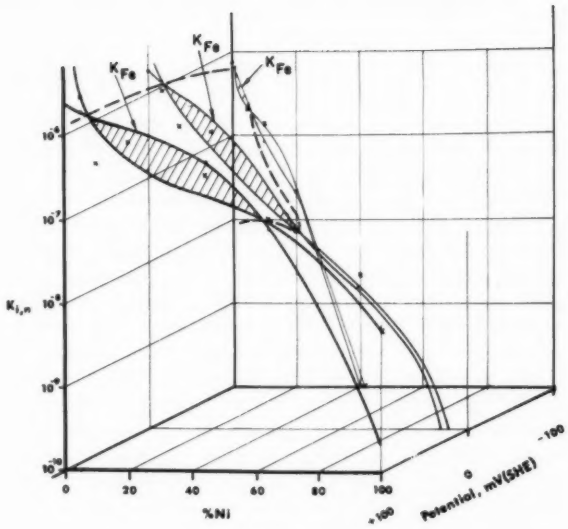

Figure 2. Intrinsic rate constants for Fe and for Ni in 1N H_2SO_4 as a function of Ni composition and potential (shaded areas indicate regions of Ni enrichment).

Lieutenant Dale O. Condit has been assigned to the Aerospace Research Laboratories since June 1968. His current research in the Metallurgy and Ceramics Research Laboratory concerns the corrosion behavior of Fe-Cr-Ni alloys.

Lieutenant Condit was graduated from Ohio State University in 1966, receiving both Bachelor of Metallurgical Engineering and Master of Science degrees under the combined bachelor-master-degree program. He is now completing his research and dissertation for a Ph.D. in Metallurgical Engineering.

REFERENCES

(1) Pickering, H. W. and C. Wagner, "Electrolytic Dissolution of Binary Alloys Containing a Noble Metal," *Journal of the Electrochemical Society, 114,* No. 7, 698, July 1967.

(2) Pickering, H. W., "Volume of Diffusion During Anodic Dissolution of a Binary Alloy," *Journal of the Electrochemical Society, 115,* No. 2, 143, February 1968.

(3) Pickering, H. W., "The Surface Roughening of a Cu-Au Alloy During Electrolytic Dissolution," *Journal of the Electrochemical Society, 115,* No. 7, 690, July 1968.

metallurgical studies of high-rate deformation

DRS. J. D. BOYD, G. T. HAHN
and A. R. ROSENFIELD
Metal Science Group,
Battelle Memorial Institute, Columbus, Ohio

High-rate deformation of metals is an increasingly important aspect of modern technology. It underlies the response of metals to notch impact, ballistic impact, and crack propagation, as well as to explosive forming and other fabrication processes. (1) Accordingly, AFOSR is supporting research at the Columbus Laboratories of Battelle Memorial Institute in order to delineate the fundamental mechanisms of the high-rate plastic deformation of metals.

It is well known that plastic deformation is accomplished by the creation, multiplication, and motion of crystal defects known as dislocations. (2) Dislocations do not distribute themselves either randomly or evenly throughout the metal; they tend to collect in arrays called slip bands (Figure 1). The procedure adopted at Battelle is to examine these slip bands in detail by high-resolution

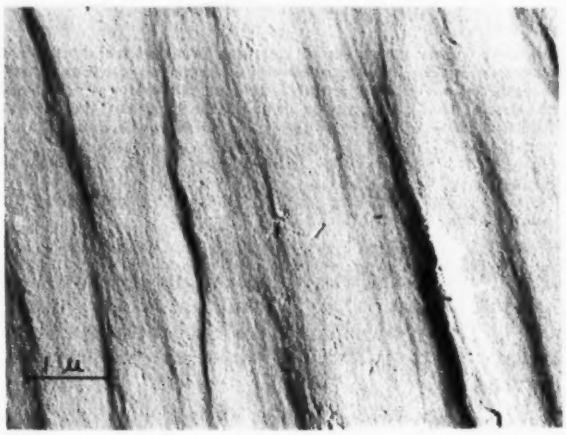

a

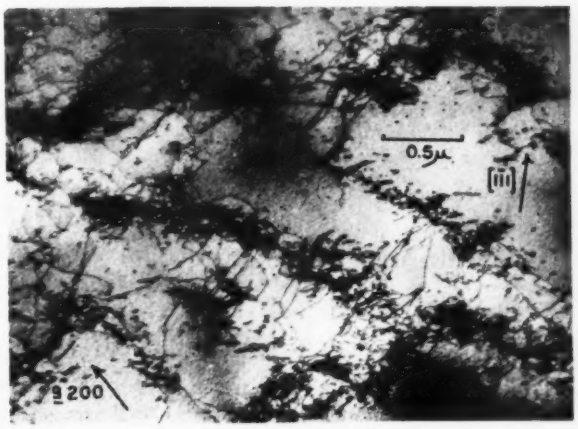

b

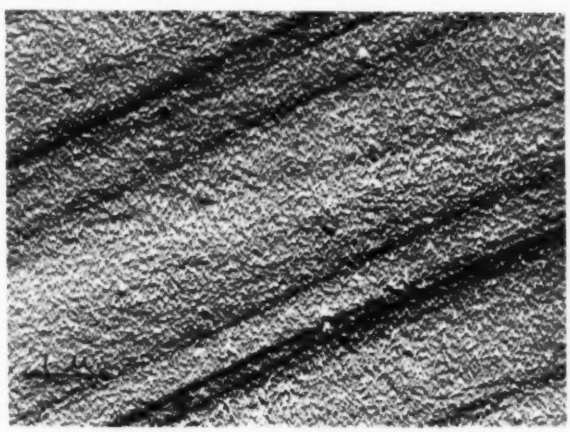

c

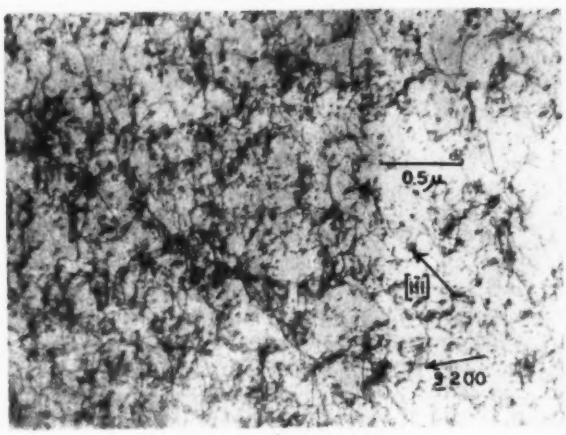

d

Figure 1. Slip bands and dislocation substructures in niobium deformed 15 percent at 2 different strain rates: (a) strain rate = 10^{-4} sec.$^{-1}$, surface replica showing wavy slip bands; (b) strain rate = 10^{-4} sec.$^{-1}$, transmission micrograph showing walls of dislocations in primary slip plane; (c) strain rate = 10^{3} sec.$^{-1}$, surface replica showing straight slip bands; (d) strain rate = 10^{3} sec.$^{-1}$, transmission micrograph showing uniform distribution of dislocations in the primary slip plane. There is a preponderance of screw-dislocation segments.

electron microscopy and relate their structures to changes in strength. For example, Edington (3) examined niobium (columbium)* samples deformed at rates from 10^{-4} to 10^{+4} sec^{-1}. He found that the yield stress at the low strain rates is not only less sensitive to rate changes than at high strain rates, but also that this change in rate sensitivity is accompanied by a distinct change in dislocation structure in the bulk of the sample (as observed by transmission electron microscopy).

Simultaneously with these experiments, work was begun to examine surface slip markings by means of plastic replicas. Surprisingly enough, at the onset of this program, almost no high-resolution surface observations had been made of the deformed surfaces of the technologically important body-centered-cubic metals, despite the large number of bulk observations. The two kinds of observation are complementary: transmission microscopy reveals the current structure of the slip band, while surface replicas provide a record of the strain that has been accomplished within the band.

High-resolution slip-line studies of iron and steel deformed at low strain rates over a range of temperatures were reported early this year. (4) At that time, the limit of resolution (i.e., the finest detail observable) was ~ 200 Å. Recently, by going to the so-called single-stage technique, this limit has been reduced to ~ 60 Å (~ 25 atomic spacings). Furthermore, these studies are now being made quantitative by means of the latex-ball technique described in the caption for Figure 2. This technique, used previously by workers at the Max Planck Institute in Stuttgart, allows one to determine the local strain in each slip band. For example, in the Figure 2 sample, the band is roughly as broad as it is deep, indicating a local strain of about 1.0, while the average strain in the specimen is close to 0.2.

A second way of making the observations more quantitative is to use single crystals, since the plane and direction of motion of dislocations can be determined. Together with the latex-ball studies, the geometry of slip can be well characterized. This procedure is now being applied to niobium crystals tested in three ways: low-strain-rate at either room temperature or -196° C, and high-strain-rate at room temperature. Furthermore, the room-temperature, high-strain-rate structure corresponds to the cryogenic-temperature, low-strain-rate structure.

As a result of these experiments, a clearer picture of the deformation process is beginning to emerge. Apparently, the slip bands form early in the deformation process (at strains less than 1%). They cause detectable offsets of the metal surface, with the arrangement of the remaining dislocations depending on the testing conditions (see Figure 1). At low-strain rates and room temperature, a disproportionate amount of dislocation motion is localized at or near the existing bands, causing the surface offsets to become larger and more distinct. At the same time, some strain occurs in the region between existing slip bands. At high-strain rates and/or low temperatures, the evidence is not as clear. However, the situation appears to be reversed, with the tendency for filling in the regions between existing bands greater than the tendency to concentrate slip within existing bands.

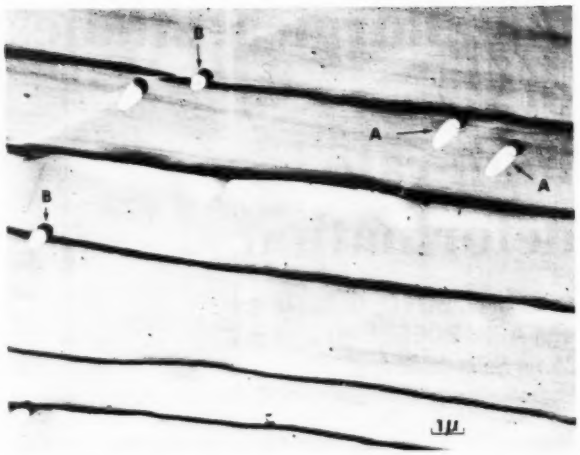

Figure 2. Strain measurement with the latex-ball technique.—The technique involves electropolishing a sample to produce a very smooth finish. After the sample is strained, a carbon replica is made of the surface. This replica faithfully reproduces the surface structure, even to very fine details. After the small latex balls are placed on the replica, a film of Pt-C is evaporated onto it to highlight the features. The shadows cast by the balls can be measured. In this case, shapes of the shadows of balls labeled "A" indicate that the shadowing angle is ~ 20%, while those labeled "B" indicate a step height of 0.2 μ.

The physical reason for this action is thought to be in the behavior of screw dislocations, which tend to move in straight lines. However, given sufficient time and thermal agitation, their paths will become very erratic, due to a process known as cross-slip. This effect shows up nicely in the surface observations, since the slip bands are the traces of the paths of screw dislocations.

In summary, a qualitative basis for understanding high-rate deformation is emerging. The experiments necessary to make this picture quantitative have been undertaken. These have the eventual goal of providing the very complex links between the response of the metal as a whole to impact and the behavior of the dislocations which cause the metal to deform.

REFERENCES

(1) For a state-of-the-art survey on high-rate deformation, see U.S. Lindholm, ed., *Mechanical Behavior of Materials Under Dynamic Loads*, Springer-Verlag, New York, 1968.

(2) Two good introductory books on dislocation theory are (a) D. Hull, *Introduction to Dislocations*, Pergamon Press, London, 1966, and (b) J. Weertman and J. R. Weertman, *Elementary Dislocation Theory*, MacMillan, New York, 1964.

(3) Edington, J. W., "Effect of Strain Rate on the Dislocation Substructure on Deformed Niobium Single Crystals," Reference (1), p. 191.

(4) Boyd, J. D., G. T. Hahn, A. R. Rosenfield and E. Votava, "Character of Slip Bands in Iron and a Mild Steel with Manganese," *Trans. ASM, 62*, 206 (1969).

** Niobium has the same crystal structure as iron and essentially the same yielding behavior. However, its use avoids several experimental difficulties which have little bearing on the problem at hand.*

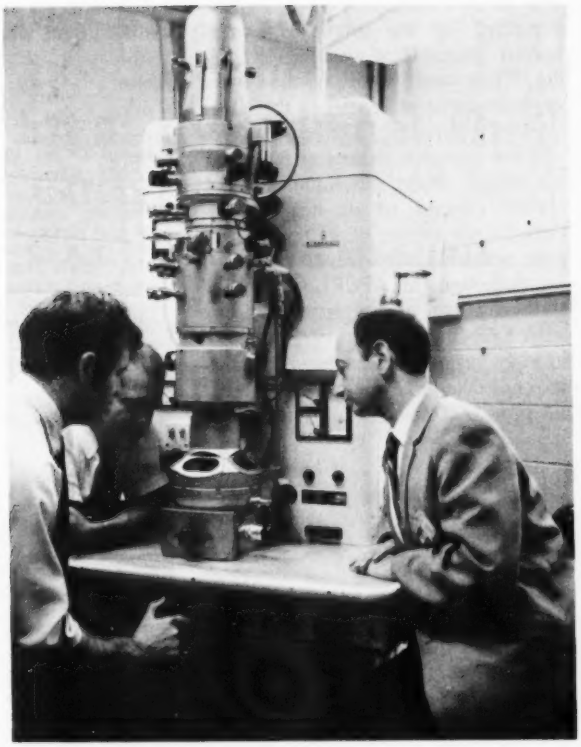

Drs. J. Douglas Boyd, George T. Hahn, and Alan R. Rosenfield (left to right) examine an impact specimen in the electron microscope at Battelle-Columbus.

Dr. J. D. Boyd received his Ph.D. from Cambridge University and joined Battelle in 1966. His thesis research was on the growth of precipitates in age-hardening aluminum alloys. Drs. G. T. Hahn and A. R. Rosenfield both received their Sc.D. degrees from MIT, Dr. Hahn joining Battelle in 1960 and Dr. Rosenfield in 1962. They have worked extensively on the metallurgy and mechanics of structure.

Among them, the three researchers have authored about 80 papers in the scientific literature. They are members of the major metallurigical professional societies.

WATER IN A VACUUM AND LUNAR RIVERS

SPACE PHYSICS LABORATORY, AFCRL

In an article appearing in *Science* last year, Richard E. Lingenfelter of UCLA suggested that the sinuous rills observed on the moon were the result of surface erosion by water. He states that "such erosion could occur under a pressurizing ice cover in the absence of a lunar atmosphere. Water, outgassed from the lunar interior and trapped beneath a layer of permafrost, could be released by a meteoritic impact and overflow the crater to form an ice-covered river." He estimates that a rill could be eroded in about 100 years.

This is an intriguing idea because, of all the resources that man would like to find on the moon, none is more valuable than water. The Lingenfelter article prompted Dr. John W. Salisbury and Joel Adler of AFCRL's Lunar-Planetary Research Branch to put the suggestion to a test. They reported their results in the May 2, 1969 issue of *Science*. A basic question to be answered in these tests was: What happens to water when it is introduced into a vacuum?

For their tests, the AFCRL scientists used a vacuum chamber large enough to admit a 30-by-42.5-cm tray containing a layer of crushed rocks and soils simulating in particle size and composition the materials believed to exist on the lunar surface. The chamber pressure was maintained at about 1 torr, and both the soil in the chamber and the water used were at room temperature.

What happened when the water was admitted? It exploded in vigorous, almost instantaneous, boiling. Soil particles were thrown the full 50-cm length of the test chamber. After a few seconds, however, the boiling stopped and a dendritic mass of ice began to accumulate at the opening to the chamber, capping off the water supply. An ice layer formed over the soil.

The prompt formation of ice can be explained by the simple and well-known principle of evaporative cooling. When water vaporizes, the active, more energetic molecules in the water tend to escape into the vapor state. The less energetic molecules remain in the liquid. When the liquid loses a critical amount of its heat energy through the escape of its more energetic molecules, the water freezes.

Although the AFCRL tests could neither prove nor disprove Lingenfelter's rill-forming postulate, they did strongly suggest that channel forming does not take place. However, the tests did show that ice will readily form in a vacuum to a sufficient thickness to allow liquid water to exist and flow beneath it, as predicted by Lingenfelter.

Mr. Joel E. M. Adler is a general physical scientist in the Lunar-Planetary Branch of the Space Physics Laboratory, AFCRL, where he is responsible for vacuum chambers and associated equipment used in simulating conditions of the lunar surface. He also participates in research concerned with the morphology of lunar-surface features. With a 24-inch telescope which he, as the Branch project engineer, had installed, he is conducting a program of lunar and planetary photography in the visible and near-infrared.

Mr. Adler received his B.A. in Geology in 1961 from Hofstra University, Hempstead, New York. He has coauthored several articles on his studies.

Dr. John W. Salisbury, Chief of the Lunar-Planetary Research Branch, Space Physics Laboratory, AFCRL, since 1961, directs a research program on the nature of both lunar and planetary environments. His own research deals primarily with the origin of lunar-surface features and the composition and nature of lunar-surface materials.

In 1955, Dr. Salisbury received his B.A., magna cum laude, in Geology from Amherst College, Amherst, Mass., and was elected to Phi Beta Kappa. He continued his study of geology at Yale University, earning his M.S. in 1957 and his Ph.D. in 1959.

During the summer of 1955, Dr. Salisbury was employed by the Arctic Institute of North America in the geological mapping of a section of the Brooks Range in Arctic Alaska. He was also engaged in geological mapping for the Georgia Department of Mines, Mining, and Geology during the summers of 1956, 1957, and 1958.

Joel E. M. Adler (left) and Dr. John W. Salisbury obtained some surprising results when they introduced water into a vacuum system evacuated to a pressure of one torr.

buckling and postbuckling of oval cylindrical shell under axial compression

DR. JOSEPH KEMPNER *
Polytechnic Institute of Brooklyn, New York

INTRODUCTION

Over the years much attention has been focused upon the behavior of thin-walled circular cylindrical shells subjected to axial compressive end loads. As is well known, the classical theory of elastic buckling for this problem usually predicts buckling stresses disagreeing substantially with corresponding experimental results. An explanation for this behavior was first proposed by Donnell (1) on the basis of large-deflection theory. His study sparked a series of investigations which continue to the present time.

In view of the widespread industrial utilization of the circular cylindrical shell, it is understandable that comparatively little attention has been focused on parallel problems of the noncircular cylindrical shell. Such structures are of interest to designers of flight and underwater vehicles. Results of buckling studies of the oval cylindrical shell should prove to be equally applicable to cylinders designed to be circular, but which turn out to be slightly oval after fabrication, as well as cylinders designed with cross sections exhibiting considerable out-of-roundness.

The research undertaken in the present program with the support of the Mechanics Division, AFOSR, includes theoretical and experimental studies of the buckling and postbuckling behavior of oval cylindrical shells. (2, 3, 4, 5) Reasonably good agreement has been found between the results of theory and test which show, in contrast to the behavior of circular, or nearly circular, cylindrical shells that, for moderate-to-large eccentricities, elastic collapse loads of the oval cylinder are likely to be relatively insensitive to geometric imperfections.

ANALYSIS AND RESULTS

In the analytical work the basic relations applied to investigate the behavior of homogeneous, isotropic, noncircular cylinders correspond to those of the Donnell-von Karman type nonlinear theory of thin-walled shells. The analysis is based upon the principle of stationary potential energy, together with an appropriately assumed deflection function. The local radius of curvature of the noncircular cross section is taken to correspond to the family of doubly symmetric, oval cross-section cylinders whose local radius of curvature is given by the relation

$$r = r_o / [1 - \xi \cos (2s/r_o)]$$

where $r_o = L_2/2\pi$ is the average radius of curvature, and ξ, the eccentricity parameter, is restricted to range between zero and unity, corresponding in a rather complicated manner to the major-minor axes ratio (b/a) varying from 1 to 2.06; L_2 is the circumferential length of the middle surface of the shell of wall-thickness h (see Figure 1).

The classical (small-deflection) buckling stress σ_{CR}, obtained as a limiting case of the aforementioned nonlinear solution, is plotted as a function of ξ (or b/a) for several values of the average radius-to-thickness ratio r_o/h in Figure 2 ($K = [12(1-\nu^2)]^{1/2}$ (r_o/h) and ν is Poisson's ratio, taken as 0.3). The ordinate is the ratio of the classical buckling stress of the oval cylindrical shell to that of the equivalent

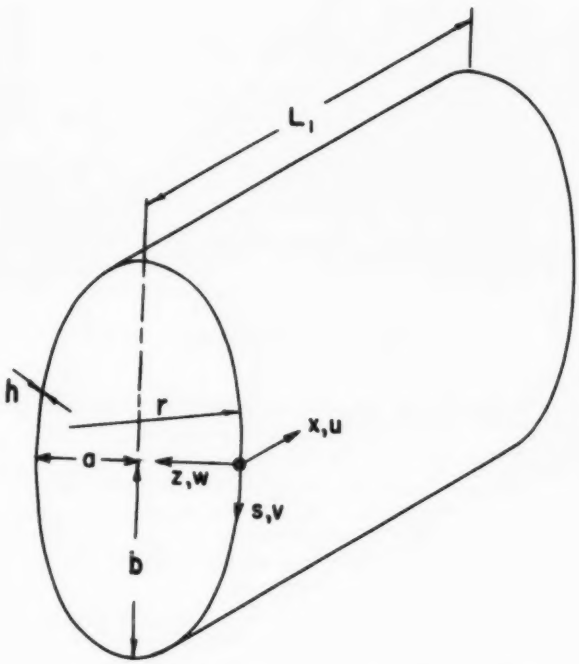

Figure 1. Sign convention and geometry.

circular sylindrical shell (the circular cylinder having the same developed surface area and thickness as its corresponding family of ovals; $\sigma^o_{CR} = 2E/K$, where E is Young's modulus). As expected, the curves show that the

Dr. Kempner is Professor and Head of the Department of Aerospace Engineering and Applied Mechanics at PIB.

out-of-roundness has a marked effect on the buckling load. For example, if b/a = 1.4 (i.e., $\xi = 0.5$), the buckling stress is reduced to 50 to 60 percent of that of the equivalent circular cylinder, the exact reduction depending upon K. The lowest curve (dashed) represents an asymptotic solution whose buckling stress coincides with the engineering approximation achieved by simply substituting the value of the maximum radius of curvature of the cross section of the oval cylinder considered into the classical buckling formula for an axially compressed circular cylindrical shell ($\sigma^*_{CR} = 0.6Eh/r_{max}$). This simple result is seen to yield good results for very thin-walled cylinders, and reasonable results for all values of r_o/h for moderate b/a ratios.

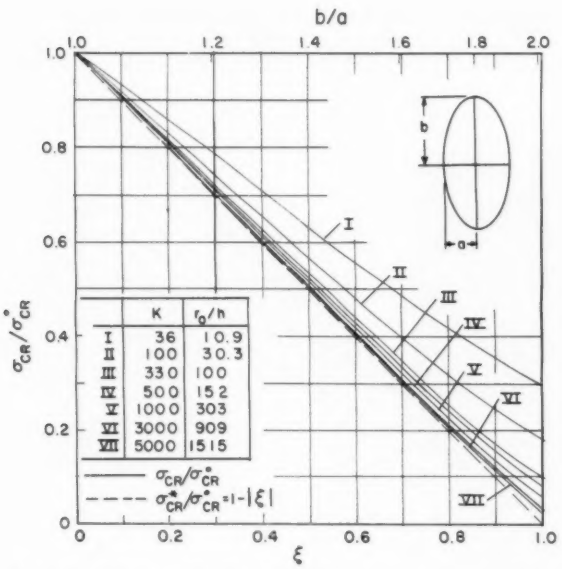

Figure 2. Variation of classical critical load with eccentricity parameter and major-minor axis ratio.

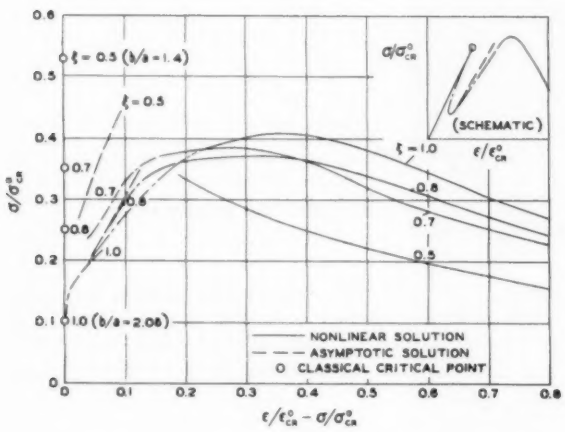

Figure 3. Theoretical response curves (r_o/h = 100, K = 330).

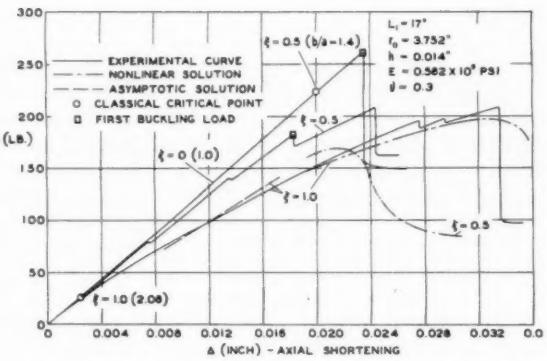

Figure 4. Experimental and theoretical response curves (r_o/h = 268, K = 884).

In the postbuckling region, the behavior of the oval cylindrical shell can best be characterized by response curves relating the applied compressive stress σ to the unit end shortening ϵ. A sketch of such a curve is shown in the inset in Figure 3, where $\epsilon^o_{CR} = \sigma^o_{CR}/E$. Figure 3 also presents typical results determined by the nonlinear analysis, including an asymptotic solution in the vicinity of the classical buckling loads. Although curves are not available for the immediate neighborhood of the bifurcation points represented by the circles, computed estimates of the bifurcation angle show that the local response is of the nature indicated in the inset.

Thus, the results suggest that, as in the well-known case of the circular cylinder, the initial postbuckling curve starts with an unstable branch which exhibits a decreasing end shortening until a vertical tangent corresponding to a minimum value of ϵ is reached. Subsequently, a first relative minimum for the applied stress σ is expected, followed by stable equilibrium states corresponding to stress increasing with increasing end shortening until a maximum postbuckling load is attained. Hence, after the first minimum load is reached, the behavior of the oval cylinder can be markedly different from that of the circular cylinder, since the latter can hardly, if ever, support a load much higher than the minimum postbuckling load once the cylinder has buckled.

Additionally, despite the similarity between the response of the circular and oval cylinders in the immediate neighborhood of the bifurcation points, it is found that the first stable branch for the oval cylinder is generally much closer to the prebuckling curve ($\sigma/\sigma^o_{CR} - \epsilon/\epsilon^o_{CR} = 0$) than that for a circular cylinder. Hence, the snap-through buckling phenomenon for an oval cylinder of even moderate eccentricity is substantially less drastic than that for a circular cylinder, while the snap-through of an oval cylinder with large eccentricity is not even noticeable. This behavior is observed in Figure 4, which exhibits experimentally determined response curves for mylar cylinders with r_o/h = 268. It is interesting to note that even the moderately eccentric oval cylinder $\xi = 0.5$ (i.e., b/a = 1.4) does not show a drastic drop in load after the first buckles are

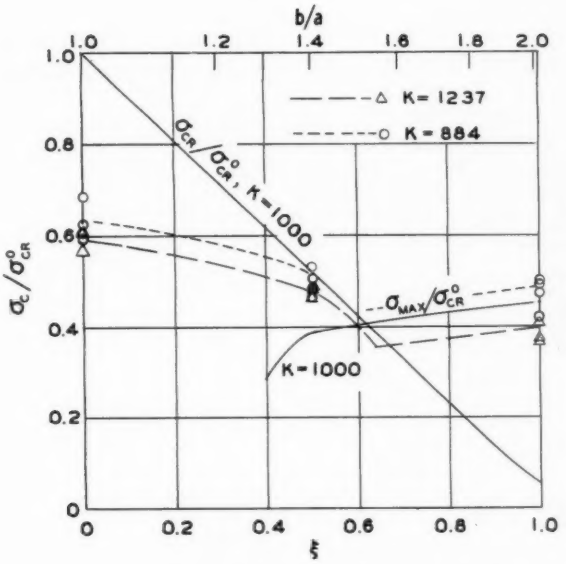

Figure 5. Comparison of theory and experiment for the elastic collapse load of oval cylinders [r_o/h = 268; 375 (K = 884; 1237)].

developed (at the ends of the minor axis). For $\xi = 1$ (i.e., b/a = 2.06), the experimental response curves extend through the region of the bifurcation point and the first minimum load without a noticeable drop and, ultimately, reach a point corresponding to as much as 8 times the classical buckling load. After such a maximum load is attained, the collapse is as catastrophic as that of a circular cylinder.

The theoretical curves shown for the oval cylinder are in surprisingly good agreement with the test records. Both the theoretical and the experimental data show that, as expected, buckles initiate in the regions at the end of the minor axis and progress to regions of greater curvature, until final collapse occurs.

In Figure 5 a comparison of theory and experiment is presented in a form that might be of use to designers. The ratio of the elastic collapse load to the classical buckling load of the equivalent circular cylinder is plotted against the eccentricity parameter, ξ. The data cover 21 test cylinders. Theoretical results for K = 1000 (r_o/h = 303) are given by the solid curves for the classical buckling stress of the oval cylinder (σ_{CR}) and for the maximum postbuckling stress. The broken curves simply connect the test points.

Thus, the results in Figures 4 and 5 strongly suggest that, for oval cylinders with moderate to large eccentricities, for which the maximum postbuckling load is of the order of, or higher than, the classical buckling load, the maximum load serves as a more meaningful definition of the collapse load than does the classical buckling load. On the other hand, for oval cylinders with small eccentricity, stability may be better characterized by the classical buckling load, which is now higher than the maximum postbuckling load. In this case imperfection sensitivity

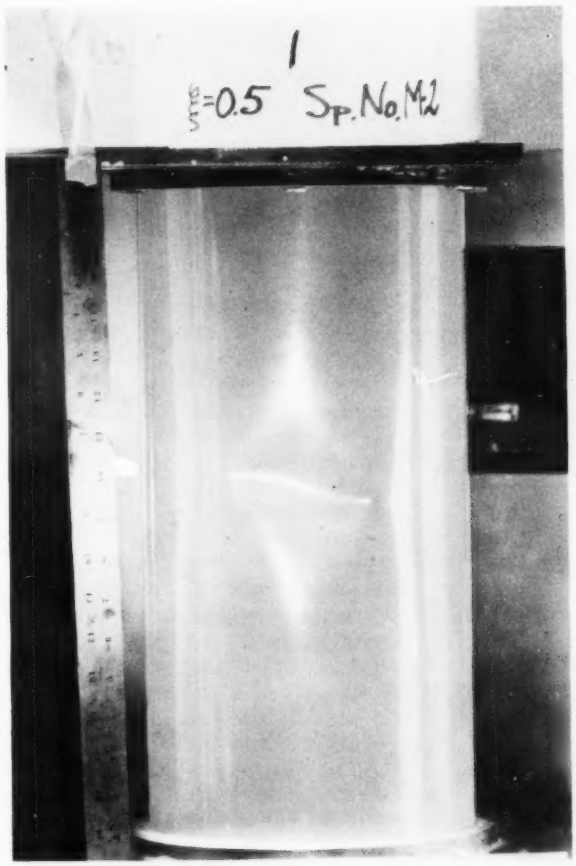

Figure 6. Initial buckling of oval cylinder.

similar to that of the circular cylinder must then be expected. Although no analytical results are currently available with regard to the sensitivity of the oval in connection with the maximum postbuckling load, the agreement between theory and experiment does suggest that, since the test cylinders undoubtedly contained unavoidable imperfection, the collapse loads of oval cylinders with moderate-to-large eccentricities are not very sensitive to initial imperfections.

The sequence of photographs given in Figures 6 to 8 characterize the several stages exhibited during the axial compression tests of the oval cylinders. In the first of these the initial buckling stage has just been reached. Buckles have formed at the ends of the minor axis in accordance with the predictions of the small-deflection (classical buckling) solution. In Figure 7, loading has advanced to the maximum stress level which, as discussed previously, can considerably exceed the classical buckling stress. Of course, the deformation has spread to the ends of the major axis where the stiffness is greatest. The last photograph shows the cylinder after collapse. It can continue to take some (reduced) load and, when unloaded, can be retested with no appreciable change in the maximum load.

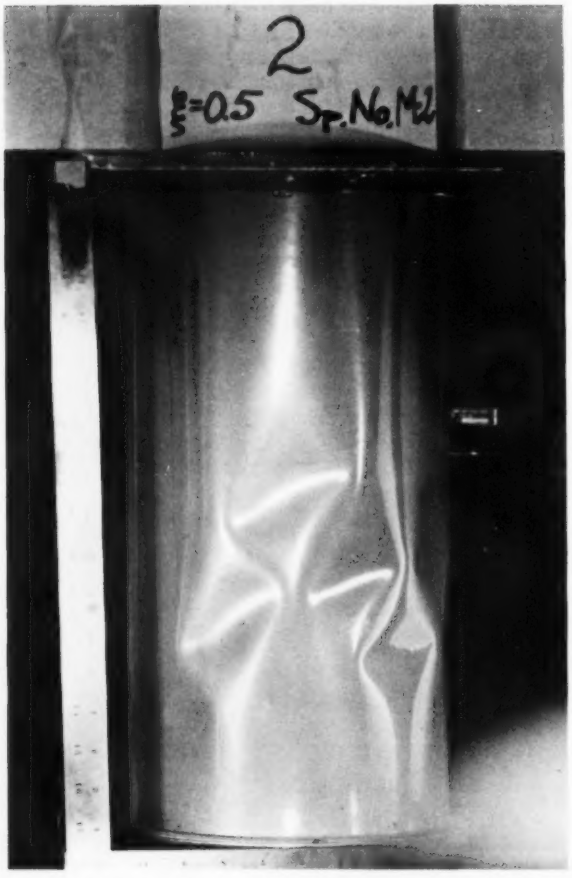

Figure 7. Deformation at maximum stress level for oval cylinder.

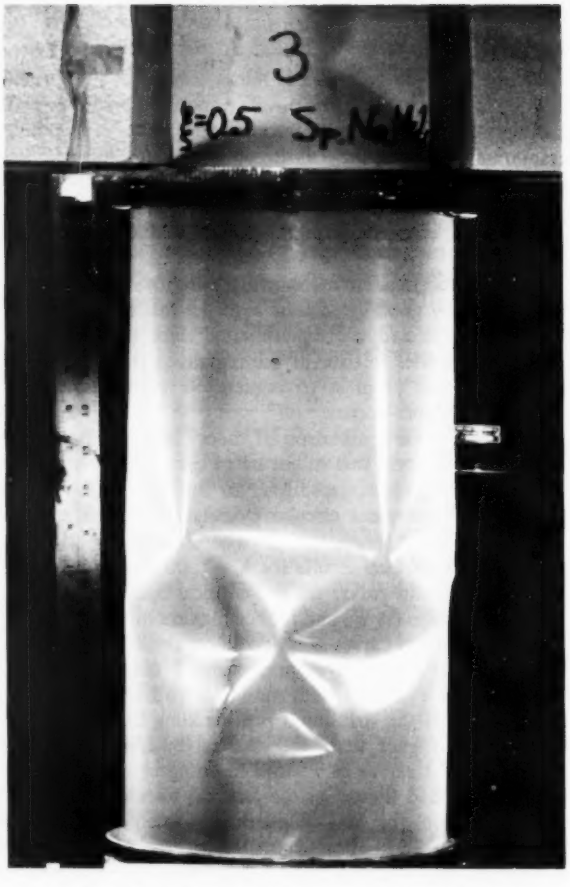

Figure 8. Deformation after collapse of oval cylinder.

REFERENCES

(1) Donnell, L. H., "A New Theory for the Buckling of Thin Cylinders under Axial Compression and Bending," *Trans. ASME*, Vol. 56, 1934, p. 795.

(2) Kempner, Joseph, "Some Results on Buckling and Postbuckling of Cylindrical Shells," *Collected Papers on Instability of Shell Structures – 1962, NASA TN D-1510*, 1962, p. 173.

(3) Kempner, Joseph and Youl-Nan Chen, "Large Deflections of an Axially Compressed Oval Cylindrical Shell," *Proc. XI Inter. Cong. Appl. Mech., Munich, Germany, 1964;* Berlin: Springer-Verlag, 1966, p. 299.

(4) Kempner, Joseph and Youl-Nan Chen, "Buckling and Postbuckling of an Axially Compressed Oval Cylindrical Shell," *AFOSR 66-0870*, Polytechnic Institute of Brooklyn, April 1966; also *Proc. Symp. on the Theory of Shells to Honor Lloyd H. Donnell*, McCutchan Pub. Co, May 1967, p. 141.

(5) Kempner, Joseph and Youl-Nan Chen, "Postbuckling of an Axially Compressed Oval Cylindrical Shell," *AFOSR 68-1944*, Polytechnic Institute of Brooklyn, November 1968; also Sectional Lecture, 12th Inter. Cong. Appl. Mech., Stanford Univ., 26-31 Aug. '68, to appear in Congress *Proceedings*.

IONOSPHERIC PHYSICS LABORATORY, AFCRL

LOW-FREQUENCY AIRCRAFT COMMUNICATIONS SYSTEM

The problem is this: to develop an aircraft communications system to operate at low frequencies. *What's so difficult about that?* The antenna; it must be about a mile and a half long if you are going to transmit at 60 kHz. *Well, if you really want to transmit at this frequency, then simply reel out a wire from the aircraft.* That's an approach, but a horizontal antenna would be extremely inefficient for LF transmissions. *You mean that your problem is to extend an 8,000-foot vertical antenna from an aircraft in flight? Impossible!*

It *is* impossible. But it's not impossible to provide an aircraft with a low-frequency transmission system, 8,000-foot vertical antenna and all. AFCRL is testing components for such a system. Behind the development of such a system is the fact that severely disturbed ionospheric conditions could completely black out air-to-ground communications at conventional aircraft frequencies. Transmissions at low frequencies, however, are not affected by such disturbed conditions.

AFCRL's idea is for the plane to carry an expendable battery-powered transmitter which is dropped from the aircraft. Before the package is dropped, the message is tape-recorded into it. After being dropped, a parachute is deployed to decelerate the transmitter gently, giving a long, slow descent to the ground. From an altitude of 45,000 feet, the descent time to sea level is nearly an hour.

As the package drops, 2 reels of wire are played out simultaneously and as quickly as feasible. One reel containing 4,000 feet of wire is dropped with an aerodynamic breaking device to control the descent. The other reel also contains 4,000 feet of wire which is extended above the central transmitter by special parachute.

When the reels are unwound, the transmitter is at the center of a vertical half-wave dipole. Being center fed, the antenna impedance is essentially resistive and low enough (90-100 ohms) to be conveniently driven by the solid-state transmitter. Electrical tests conducted at the Army's Aberdeen Proving Ground show that, with 7 strands of No. 18 copper clad cable—a standard material—the radiation efficiency is about 80 percent. Using silver zinc-batteries, transmission times on the order of 30-45 minutes and a radiated power of 3 kw should be obtainable without exceeding an overall weight of 300 pounds for the entire package.

While the various individual aspects of the device have been successfully tested, a complete working model has not yet been assembled. Work in this area has been carried out under the direction of Dr. Edward A. Lewis, at the Ionospheric Physics Laboratory, AFCRL.

Dr. Edward A. Lewis is Chief of the Electromagnetic Environment Branch, Ionospheric Physics Laboratory, AFCRL. He is currently directing a fundamental research program in the low, very-low, and extremely low frequency regions, and also directing a program of applied research to devise and develop techniques for improving USAF military capabilities. He has spent much of his career in work related to the propagation of very-low-frequency waves through the atmosphere, work that extends back to the early atomic-test program and to the study of VLF pulses emitted by nuclear detonations.

With the aid of two scholarships, Dr. Lewis spent his undergraduate years at Dalhousie University in Halifax, Nova Scotia, where he received a B.S. with High Honors in Mathematics, and subsequently his M.S. in Physics. In 1950, he received his Ph.D. in Physics from the Massachusetts Institute of Technology.

THE HYPERSONIC ROLL-DAMPING DERIVATIVE OF A BLUNT CONE

DR. BRIAN QUINN, Energetics Research Laboratory, ARL

The roll-damping derivative, C_{ℓ_p} is one of the many aerodynamic coefficients that influences the flight dynamics of a rolling missile. In general, it measures the resistance (or propensity) of the missile to rotate about its longitudinal axis. Knowledge of this derivative has been limited, especially for unfinned bodies of revolution in hypersonic flight. Accordingly, the measurement (1) and theoretical computation (2) of the roll-damping derivative of a blunt cone recently served as a focal point in the Hypersonic Research Laboratory's continuing study of the stability of vehicles in high-speed flight.

The general features of the flow field around a slightly blunted cone in hypersonic flight have been known for many years, and depart dramatically from those associated with a sharp cone. The latter, for instance, generates a conical flow field with gas properties constant along rays from the cone vertex so long as the free-stream Mach number assures an attached shock wave. In contrast, the shock wave produced by a blunted cone always separates from the body and the flow field is never conical or, at best, approaches conicity many nose diameters downstream. In brief, such flows exhibit three regimes (Figure 1). The first of these is encountered in the stagnation or

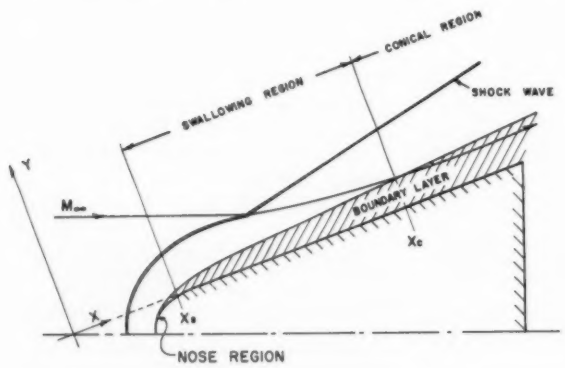

Figure 1. Schematic representation of hypersonic flow over a blunt cone.

nose region where the flow accelerates from stagnation conditions to conditions at the cone shoulder, x_s. The second regime extends from the shoulder to a point downstream called the swallowing distance, x_c. In this region, the boundary layer swallows the external entropy layer, or those streamlines that have crossed the curved part of the shock wave. In this regime, flow properties differ from one streamline to another upon entering the boundary layer because each streamline has crossed the shock wave at different inclinations. Consequently, fluid properties at the edge of the boundary layer vary from station to station. There is one streamline, however, that crosses the shock wave at a point where it is no longer curved but grows linearly with downstream distance. Where this streamline enters the boundary layer defines the swallowing distance. Moreover, all streamlines entering the boundary layer downstream of this point carry identical fluid properties because each has crossed the shock wave at the same inclination. For this reason, streamwise gradients in the fluid at the edge of the boundary layer no longer exist. This is the third regime. In the analysis of Reference 2, it was assumed that rolling the cone about its axis of symmetry in no way changed the external flow field in each of the flow regimes.

In the absence of fins, the elemental aerodynamic moment, -dL, tending to reduce the rate at which a blunt cone is spinning about its axis of symmetry, is due entirely to the peripheral component of the local skin friction acting across a moment arm equal to the local radius. The local moment, -L, is conveniently written as the sum of two parts: the integral of -dL along the surface of the spherical nose region, and the integral of -dL along the surface of the remainder of the body. For the interesting case of moderate nose-bluntness ratios, i.e., $\frac{\text{nose radius}}{\text{base radius}}$ less than around 15%, it can be shown that the contribution of the nose region to the overall moment is a negligibly small fraction of the contribution from the integral across the aft section of the cone. For the most part, this can be attributed to the combination of a small surface area and small moment arm in the nose region. In other words, although the node region determines the character of the flow field over the entire body, it contributes practically nothing to the total roll-damping moment. This observation suggests that the rolling moment of the blunt cone can be approximated by the more simple expression for the rolling moment of a fictitious body—one whose geometry is that of a pointed cone, but whose inviscid flow field could be conical, in the case of zero nose bluntness, or correspond to the "swallowing-then-conical" flow over a cone of small nose bluntness. We will see that the convenience afforded by this simplified model far outweighs any attendant penalties in accuracy.

The variation of the peripheral skin friction along the surface of the cone can be found from three-dimensional laminar boundary-layer theory. If, in the usual manner, the equations of motion are cast in the form relating stream functions and similarity variables, there results a well-defined system of equations with the appropriate boundary conditions. Linearizing the system with respect to the roll

rate considerably simplifies the problem while continuing to represent the actual flight condition. Details of the analysis may be found in Reference 2, where it is shown that the equations of motion reduce to equations with known solutions. In general, by relating the peripheral component of skin friction to known quantities, the rolling moment can be expressed as follows:

$$-L = 0.8412\, p r_B^2 (\xi_\ell)^{1/2} \qquad (1)$$

where

$$\xi_\ell = \int_0^\ell \lambda \rho_1 u_1 \mu_1 r^2\, dx$$

In the above, p is the roll rate, r_B is the base radius of the cone, λ is the proportionality constant of a linear viscosity relationship, and ρ_1, u_1, and μ_1 are the local density, velocity and viscosity coefficient at the edge of the boundary layer. Thus, computation of the rolling moment is reduced to the evaluation of a single integral.

As an example, consider the experimental values of roll-damping derivatives for a blunt-nosed 10° cone reported by O. Walchner in Reference 1. Typical wind-tunnel conditions were $T_t = 2060°R$, $P_t = 1615$ psia, $M_\infty = 14.25$, $T_o/T_t = 0.31$ and, based on a cone diameter of 5 inches, $R_{e_\infty} = 0.241 \times 10^6$. Results measured at $pr_B/u_\infty = 0.0053$ were indistinguishable from those at 0.003. With these conditions, equation (1) can be used to give

$$c_{\ell_p} = \frac{\delta c_\ell}{\delta\left(\frac{pr_B}{u_\infty}\right)} = \frac{\delta}{\delta\left(\frac{pr_B}{u_\infty}\right)}\left[\frac{L}{\rho_\infty u_\infty^2 \pi r_B^3}\right] = 0.0093\left(\xi_\ell\right)^{1/2} \qquad (2)$$

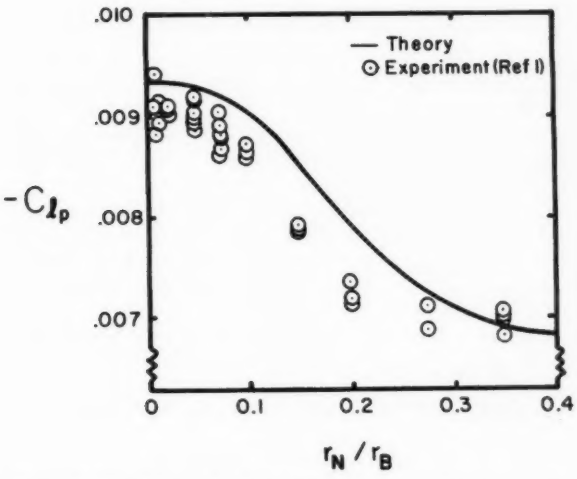

Figure 2. Dependence of roll-damping derivative on bluntness ratio.

Equation (2), computed by simple graphical integrations for the ξ_ℓ's, has been drawn in Figure 2 along with the experimental values of c_{ℓ_p} from Reference 1. The theoretical and experimental results exhibit the same trend for increasing nose bluntness and agree to within a few percent over the range $o \leq r_N/r_B \leq 0.4$. For bluntness ratios much greater than this, the validity of neglecting the nose-region's contribution to the roll-damping moment as well as other theoretical simplifications becomes questionable. Within the limit of small nose bluntness, however, the theory reasonably predicts the moderate loss in roll damping. In contrast with this result, it may be of interest to recall earlier ARL studies (3,4) which show a rather drastic reduction in the pitch-damping derivative of spherically blunted cones in hypersonic flight.

REFERENCES

(1) Walchner, O., "Laminar Hypersonic Roll-Damping Derivatives for a 10° Cone," *AIAA Journal*, 7, 2, 342-344, 1969.

(2) Quinn,B., "The Hypersonic Roll-Damping Derivative of a Blunt Cone," *ARL 68-0137*, 1968.

(3) Walchner, O. and J. T. Clay, "Nose-Bluntness Effects on the Stability Derivatives of Cones in Hypersonic Flow," *Transactions of the Second Technical Workshop on Dynamic Stability Testing* (AEDC, ARO, Inc., Arnold Air Force Station, Tenn.) Vol. I, Paper 8, 1965.

(4) Quinn, B., "A Destabilizing Effect of Severe Nose Bluntness," *J. of Spacecraft and Rockets, 4,* 1388-1390, 1967.

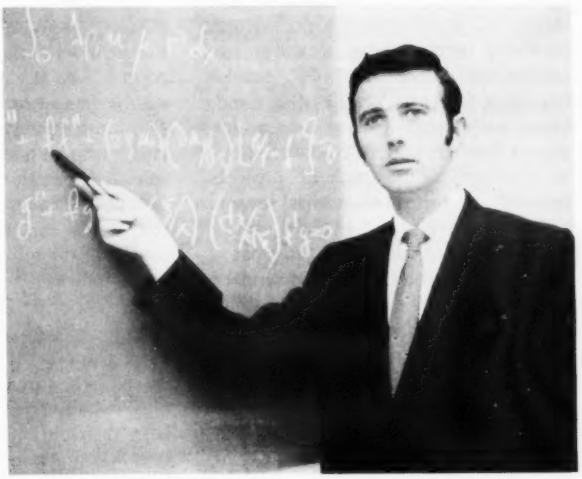

Dr. Brian Quinn was assigned to the Energetics Research Laboratory, ARL, in September 1967 as an aerospace engineer (flight and fluid mechanics) after having completed a three-year tour of active duty as a 1/Lt USAF with ARL's Hypersonic Research Laboratory. Prior to that, from September 1962 to June 1964, he held the position of "chercheur" at the Laboratoire de Mecanique des Fluides, Centre Orsay while a doctoral candidate at the University of Paris, France.

During the summer of 1962, Dr. Quinn was a research engineer with the Grumman Aircraft Engineering Corporation, Bethpage, Long Island, New York. His principal duties involved force measurements on models of reentry configurations in Grumman's shock tunnel.

Dr. Quinn has a B.S. in Engineering from the University of Notre Dame (1959), master's degrees in both Aeronautical Engineering (Notre Dame, 1962) and Business Administration (Miami University, 1968), and a PhD from the University of Paris (1964).

LA VERNE E. WOODS
Research Information Office
AFCRL

on heating an electron

Futurists are enjoying a kind of vogue. These are the people–Herman Kahn of the Hudson Institute is the archetype–who amass a multitude of situational data, correlate and analyze it for relationships, assign weighting factors, and then extrapolate to some future condition.

Let us enter the game with the following problem in mind: we want to know where we will have arrived 100 years hence in the art of weather prediction. We are not very good at weather prediction now, in 1969. We are just beginning to gain full respect for the matrix of interconnected and dynamically varying factors. It doesn't take a futurist of great analytical astuteness to foresee that weather forecasting in the year 2069 will be done numerically. Only computers can assimilate and correlate all the many synergetically reinforcing factors. Even now we are making some penetrating exploratory forays into the field of numerical forecasting.

Nevertheless, to the meteorologist looking back from the year 2069, our art is very primitive, based as it is largely on gross tropospheric features involving temperatures, pressures, humidity and circulations. His precise two-week forecasts, on the other hand, begin with solar observations which permit him to predict future variations in solar emissions; these he projects forward in terms of auroral events which add heat to the upper atmosphere, of ozone-formation rates based on solar ultraviolet variations, and of the chemical and physical processes in the upper atmosphere which also contribute heat. Because he has such a clear understanding of the casual chain of events that initiate and sustain weather patterns, the future meteorologist must wonder at the gropings of those who now are trying to discern the nature of what, to him, must seem like relatively simple relationships.

But to us in 1969 they are not simple. They are remarkably complex, and most complex of all are the heating processes of the atmosphere above the mesopause beginning at 80 km or so. This region contributes only minutely to the energies of the earth's weather; but future meteorologists may find them critical in their long-range forecasting criteria. In 1969, the meteorologist must ignore this heating source if he is to make any progress at all. He has all he can do to understand the more massive energy generation and transport phenomena in the troposphere and stratosphere.

In any event, the present-day meteorologist can always glance over to see if anything of possible meteorological significance is being uncovered by the upper-atmospheric physicists. Let us now refocus our attention on the lagging upper-atmosphere phase of meteorology. Upper-atmosphere physicists–whether their specialty is in electron distributions, atmospheric densities, chemical processes, hydromagnetics, ultraviolet absorption, or any one of many others–are all concerned directly or indirectly with collisional processes. Many things happen in collisions. For example, a photon collides with a molecule and dislodges an electron, and the resultant ion molecule collides with an atom to form a brief association that is sundered in a collision with another particle; and so on and on, in an infinite minuet. In the process, heat is absorbed and exchanged.

Depending on his specialty, each upper-atmosphere physicist brings to bear his own set of analytical tools. One such set permits the physicist to look at the upper atmosphere as a partially ionized plasma. By way of example–one that is interesting in its own right–we have a recent AFCRL paper, "Heating of the Ionosphere and Attenuation of the Equatorial Hydromagnetic Wave," by C. W. Dubs, Dr. B. Prasad and Dr. H. H. Sen. This paper may represent a small step–one of many that must follow on the way to weather prediction in 2069. In this paper the authors consider the velocities of the particles in the collisional and heating processes of the upper atmosphere. Whether a particle will collide with another and produce a given reaction is dependent on the relative velocities of the particles. The AFCRL paper emphasizes this point. Now if you assume a uniform gas and a constant collision rate, you will get one answer. When you have charged particles moving in relation to the earth's magnetic field, you get a slightly different answer because you have a condition for systematic collisions among particles.

The authors deal with two distinct ionospheric heating methods. One involves hydromagnetic or Alfvén waves. These waves are nothing more than instabilities of the earth's magnetic field lines. Charged particles tend to stick to these lines, and the lines and associated particles vibrate at frequencies in the .01 to 10 Hertz range. These waves are dampened as the particles forming the wave collide with other atmospheric particles in a velocity-dependent, rather than a random, manner. As the hydromagnetic wave is dampened, heat is added to the atmosphere. During magnetic storms, the heating rate by this process is greatly accelerated. This concept is not new; but the AFCRL paper provides a more rigorous analysis of the amounts of heat produced than was provided previously.

The other aspect of the study–one that is new–deals with a temperature anomaly which has bothered theorists for some time because it seems to violate what we think we know about gas behavior. The anomaly is that, at certain altitudes, the tempera-

tures of electrons in the upper atmosphere are higher than the ambient gas. This anomaly is explained in terms of charge separation. When charged particles are carried along in a wind stream perpendicular to the earth's magnetic field, electrons in the wind stream are deflected in one direction and ions in the opposite direction. This creates charge separation, and thus an electric field. The three AFCRL authors show that this electric field can heat the electrons and sustain the electron temperatures significantly above the gas temperature, and that the electric field is more than enough to compensate for electron cooling by inelastic collisions with neutral molecules.

With this, we shall return to our futurist game in which we have assumed that error-free, long-range forecasts will be a part of the 2069 scene. If our assumption is correct, then studies such as that just described must surely find their way into prediction criteria, however small the hydromagnetic heat contributions may be.

But another futurist may perform his analysis under a different set of assumptions, and thus see the precise long-range forecasting problem as having such complexity that it will never admit to solution. Do we then say that the Dubs-Prasad-Sen study is an interesting analytical exercise promising nothing of value?

To answer this, we might consider another futurist projection centering around the problem of where we shall have arrived in 2069 in the art of electromagnetic sensors and communications systems. We start with the knowledge that electromagnetic radiation attenuation and environmental noise are basic considerations in the design of these future systems.

We shall stop here. There is no need to develop this and other possible projections further since, by now, the conclusion has emerged and is apparent. It has to do with the universality of application of the discoveries of basic science and the fact that, if we want to arrive at some destination tomorrow, we must do many not-clearly related things today. This evident conclusion has been stated with varying degrees of elegance many, many times. But because so much is competing for everyone's attention, this simple truth must be continuously restated to assure that it is not lost or downgraded in the scheme of things.

Mr. La Verne E. Woods has been Chief of the Research Information Office, AFCRL, since 1961. He has been associated with the information programs of AFCRL since 1955, when he was responsible for the Electronics Research Directorate's technical publications program. In his present position, he is responsible for internal and external information functions, for special reporting, protocol, the AFCRL history, and the writing, design, and editing of many of the AFCRL publications.

After World War II, Mr. Woods attended the State University of Iowa, receiving his B.A. in English in 1949, and his M.A. in Economics in 1950. His M.A. thesis, "Survey of U.S. Industrial Publications," representing a comprehensive survey of the editorial policies, the backgrounds of editorial staffs, the formats, and the costs of some 2,500 periodic company publications, was the first study of its type ever made, and was widely quoted in the business press.

Mr. Woods was a B-17 pilot during World War II with the Eighth Air Force. Shot down on his 14th mission in 1943, he spent 18 months in a prisoner-of-war camp in Germany. After his graduation from college in 1950, he joined the Office of Defense Mobilization in Washington, D.C., a new agency set up with broad powers to manage the industrial-mobilization effort during the Korean War. He was speech writer for Mr. Charles E. Wilson (of GE) who headed the mobilization program, and for other officials in the mobilization program. Mr. Woods was also coauthor of the first definitive report on the Korean mobilization program, Building America's Might, and served briefly on the staff of Secretary of Commerce Sinclair Weeks in the first Eisenhower administration.

From 1953 to 1955, Mr. Woods was with the MIT Lincoln Laboratory where he authored the scripts for the documentary films, "Counter-Balance," and "SAGE." He was also editor of the short-lived Lincoln Laboratory magazine, Scan, publication of which was suspended when he left the Laboratory.

MAGNETIC FREEZE-OUT: The role of impurity density fluctuations

DR. L. J. NEURINGER
Francis Bitter
National Magnet Laboratory, MIT

Under ordinary circumstances, in semiconductors with shallow donor levels, such as InSb and InAs, the donor levels are merged with the conduction band, even at relatively low impurity concentrations. However, at temperatures of liquid helium and below *and* in the presence of an intense magnetic field, H, the impurity levels may be caused to lie below the conduction band by an amount, ϵ_b, the binding energy. The intense magnetic field acts to shrink the electronic wave function into a volume which is comparable to, or less than, the average volume occupied by an impurity ion. As a result a bound state is formed due to the presence of the magnetic field, and the binding energy, ϵ_b (H), of this state increases as H becomes greater. In this domain, if ϵ_b is greater than the thermal energy, kT, free-charge carriers will "freeze-out" of the conduction band into the impurity bound states. This magnetic freeze-out phenomenon, which affects the equilibrium population of free-charge carriers, n_c, is observed as an increase in the Hall coefficient $R(H) \sim 1/n_c$ with the magnetic field, according to the relation $R(H) \sim \exp(-\epsilon_b/kT)$.

Recent experiments of magnetic freeze-out in n-type InAs, carried out at the Francis Bitter National Magnetic Laboratory at MIT by Dr. L. J. Neuringer and L. A. Kaufman(1), have uncovered for the first time evidence of the role played on the freeze-out phenomenon by statistical fluctuations in the impurity density. Using a recirculating He^3 cryostat specially designed for the experiments, and d-c magnetic fields up to 210 kG, Neuringer and Kaufman measured the temperature and magnetic-field variations of R(H) in samples of n-InAs ($0.9 \times 10^{16} < n \leq 2 \times 10^{16}$ cm^{-3}) over the range 0.5-4.2°K and deduced values of ϵ_b(H). They found that the magnitude of ϵ_b in this material is considerably less than present theoretical estimates of ϵ_b. More significantly, in the freeze-out domain, for fixed H, they found that, as the temperature is progressively lowered, the free-charge-carrier concentration decreases initially, but ultimately approaches a constant value at the lowest temperatures. These observations cannot be understood solely in terms of a model which pictures a sharply defined impurity level moving away, with increasing H, from a well-defined conduction band edge, since according to such a model n_c should become vanishingly small as $T \to 0$.

The experimental results may be accounted for qualitatively if it is assumed that the impurity level density of the energy states has a finite width, say Γ, and that the conduction band has a tail which extends into the forbidden gap. Such broadening of the energy level spectrum may arise from local statistical fluctuations in the impurity density within the sample. The effect of a locally higher-than-average impurity concentration is to impart a local lowering of the potential, and vice versa. The presence of such a randomly fluctuating potential causes a radical change in the density of energy states, as shown in Figure 1 for the impurity level and conduction band in n-type InAs. The binding energy $\epsilon_b^{theor.}$ predicted by present theories, which neglect fluctuation effects, corresponds to the energy difference between a well-defined impurity and a conduction band edge. However, the tail on the conduction band and the broadened impurity level act together to *decrease* the experimentally observed thermal energy gap to a value ϵ_b^{exp}, as shown in Figure 1. From the experiments and the model shown in Figure 1, Neuringer and Kaufman have obtained an estimate of the average value of the fluctuating potential Γ. Furthermore, the approach of n_c to a constant value at $T \to 0$ can be understood, in terms of the model in Figure 1, as arising from a small but finite overlap of the impurity and conduction band densities of states even at the highest

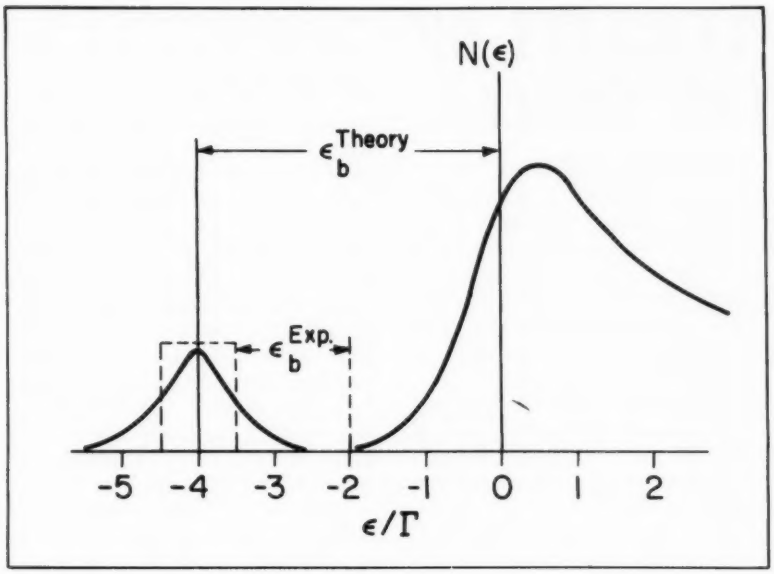

Figure 1. A randomly fluctuating potential, Γ, causes a radical change in the density of energy states, N(ϵ), for the impurity level and the conduction band in n-type indium arsenide (InAs).

magnetic fields and lowest temperatures.

A model of a heavily doped semiconductor in the freeze-out domain, such as described above, was recently proposed(2), and the experiments of Neuringer and Kaufman were undertaken to check its validity. The experimental values of the magnetic binding energy in n-type InAs and the fact that $n_c \rightarrow$ constant as $T \rightarrow 0$ are strong evidence for the presence of effects arising from statistical fluctuations in the impurity density. Values of Γ, the average value of the fluctuating potential, have been deduced from a qualitative model; they are consistent with the temperature and magnetic-field variation of n_c, and agree in order of magnitude with theoretical estimates.

REFERENCES

(1) This work represents a portion of a dissertation submitted by L. A. Kaufman to the faculty of Tufts University in partial fulfillment of the requirements for the Ph.D. degree.

(2) Dyakonov, M. I., A. L. Efros and D. L. Mitchell, *Phys. Rev.* (to be published).

Dr. L. J. Neuringer is a senior physicist at the Francis Bitter National Magnet Laboratory located at the Massachusetts Institute of Technology. He received the B.S. degree in Physics from Rensselaer Polytechnic Institute in 1951, and the Ph.D. degree in Solid-State Physics from the University of Pennsylvania in 1957. From 1957 until 1963 he was employed at the Raytheon Research Division where he was engaged in research on the properties of infrared detectors and the fundamental noise mechanisms which limit their detection capability. He was also directly responsible for the synthesis and characterization of various III-V compound semiconductors.*

At the National Magnet Laboratory, Dr. Neuringer has investigated experimentally the basic mechanisms which limit the magnitude of the upper critical field of superconductors and the dynamics of the mixed state. At present, he is engaged in studies of quantum limit transport phenomena in semiconductors at low temperatures, and is involved in the construction of an He^3-He^4 dilution refrigerator.

Dr. Neuringer is a Fellow of the American Physical Society, and a member of the American Association for the Advancement of Science and of Sigma Xi.

*(The Francis Bitter National Magnet Laboratory is operated by the Massachusetts Institute of Technology, and is sponsored by the Solid State Sciences Division of AFOSR under contract No. F44620-67-C-007. The high-field facilities are made available to visiting researchers from institutions throughout the world.)

AEROELASTIC STABILITY OF THIN CYLINDRICAL SHELLS

DR. JACOB POMERANTZ
Directorate of
Engineering Sciences, AFOSR

The complex problems of panel flutter and divergence, and panel response to aerodynamic noise and turbulence, become one of practical consideration in the design of skin panels on aerospace vehicles and high-performance aircraft and missiles. Although preliminary design criteria are evolving for flat panel elements, very little design information is currently available for thin-walled shell-type structures. AFOSR-sponsored research at the University of Texas, under the direction of Dr. R. Stearman, embraces a combined experimental and analytical program to establish preliminary design criteria for estimating the aeroelastic stability and forced-response characteristics of thin-walled shell structures. This program includes the basic development and experimental evaluation of suitable methods of analysis.

Most current research has been concerned with investigating the aeroelastic stability characteristics of isotropic thin-walled circular cylindrical shells. Experimental studies supported by the Propulsion Wind Tunnel Facility of the Arnold Engineering Development Center (AEDC) have been conducted in the AEDC facility over the Mach number range 1.2 to 4.5 with the model shown in Figure 1. This is an ogive cylinder model with a circular arc nose; it is approximately 12 feet in length and 16 inches in diameter. The thin test shells are mounted on the circular cylindrical section near the base of the model. A boundary-layer control system, located in the nose cone of the model, is used to vary the boundary-layer characteristics over the thin test shell. The test shells could be internally pressurized and/or loaded axially to simulate various membrane stress states. Observations have been made on the influence of the viscous boundary layer, the Mach number, and the internal stress levels on cylindrical shell panel flutter. In addition, the influence of a supersonic flow field on the elastic stability of thin cylindrical shells has been studied experimentally. Theoretical investigations have also been conducted on the influence of a supersonic flow field on the elastic stability of thin cylindrical shells, and the influence of initial geometric imperfections and pre-stress induced deformations on the aeroelastic stability of the shell.

Both experimental and analytical studies on the influence of a supersonic flow field on the elastic stability (critical buckling load and mode shape) of thin-walled circular cylindrical shells indicate no significant effect. This fact is illustrated by the experimental data, shown in Figure 2, plotted against the classical buckling-load interaction parameters. The shaded points represent data from still-air buckling tests conducted on these shells, while the open symbols represent wind-tunnel test points. The flow conditions and radius-to-thickness ratios of each shell are indicated beside each test point. All the tested shells had a length-to-radius ratio of two. The triangular symbols represent dynamic instabilities (panel flutter), while the remaining open symbols represent static divergence (buckling) instabilities in the presence of an air stream. The interaction curve in Figure 2 indicates that no significant shift occurs in the wind-tunnel buckling-load points (open non-triangular symbols) when compared to their still-air buckling counterparts (dark symbols). The interaction design curve, suggested by V. I. Weingarten, constitutes a reasonable design criterion, except possibly at high internal pressures where it may be slightly unconservative. It seems plausible that a subsonic Mach-number flow field may have a more significant influence on the elastic stability characteristics of thin-walled cylindrical shells since, in this flow range, the pressure distribution tends to be more in phase with the deformation wave form. This problem is currently under investigation.

Preliminary experimental studies on the effects of the viscous boundary layer on cylindrical shell panel flutter were also conducted. During the course of this study two distinct types of panel flutter occurred at a given

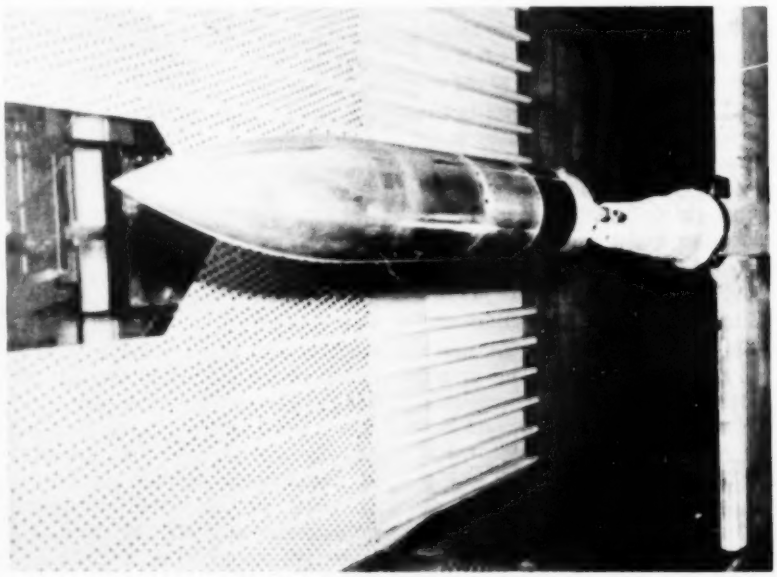

Figure 1. Ogive-cylinder wind-tunnel flutter model.

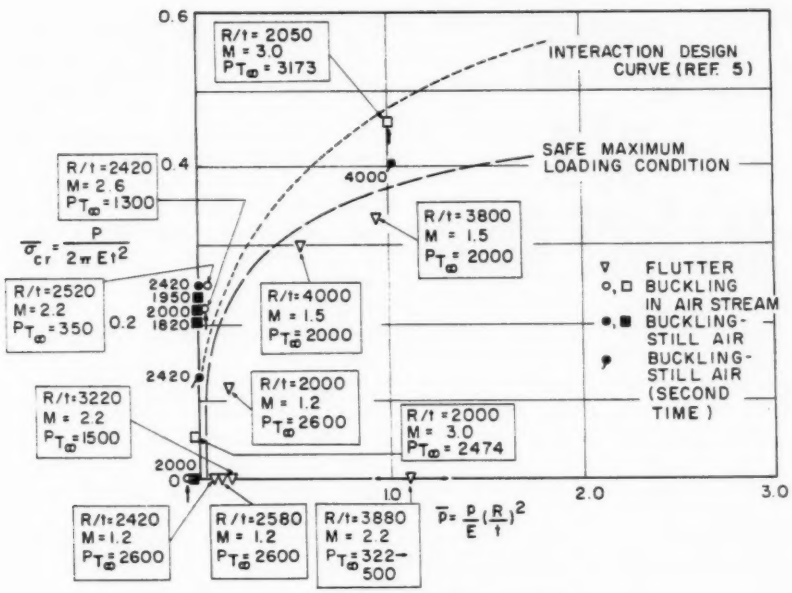

Figure 2. Buckling interaction curves and loading conditions on aeroelastically unstable shells.

Mach number. A nondestructive limited amplitude flutter occurred when the boundary layer over the shell was laminar or nearly laminar. In contrast, panel flutter in the presence of a turbulent boundary layer was always catastrophic, that is, the shells were always destroyed by the large amplitude motion within one or two seconds after its onset. It was also observed that the nondestructive limited amplitude flutter could be completely stabilized by tripping the near-laminar boundary layer, and making it turbulent and thicker. Once this turbulent boundary prevailed over the model, the catastrophic flutter could be induced, but only at much higher levels of dynamic pressures for a given Mach number. These preliminary findings indicate that the viscous boundary layer has a significant influence on cylindrical shell panel flutter. Although Y. C. Fung had hypothesized this effect earlier, this is the first time it has been demonstrated experimentally.

Additional theoretical investigations have looked into the influence of initial geometric imperfections and pre-stress induced deformation (pre-stability deformations) on the aeroelastic stability of the shell. When initial stresses are applied to an otherwise perfect shell fastened at its ends, deformations are induced by the loading condition so that the shell surface is no longer cylindrical. The more classical shell-stability studies ignore this deformation condition and consider the stability of the shell around its freely expanded or undeformed cylindrical state. When stress-induced deformations are considered, however, the shell stability is investigated about its naturally deformed state. Our analytical studies indicate that, for shells of moderate radius-to-thickness ratios (say 500 or less), a significant stabilizing influence may be induced by considering the effects of pre-stability deformations on an otherwise perfect shell. In contrast, for shells of large radius-to-thickness ratios, the pre-stability deformations are restricted to a narrow zone or boundary layer at the ends of the shell and do not significantly influence the shell's stability characteristics. Thus, the effect of pre-stability deformations will be significant only for that combination of loading and geometric parameters which cause these deformations to propagate well into the shell interior, that is, to at least 20% or more of the shell length. Further theoretical investigations indicate, however, that the combined influence of initial geometric imperfections and pre-stability deformations have a significant destabilizing influence on the aeroelastic stability boundaries of even those shells with large radius-to-thickness ratios. Consequently, the influence of initial geometric imperfections must be considered in these studies.

In summary, the present research shows that the aeroelastic stability characteristics of thin cylindrical shells are influenced by many parameters which significantly complicate the problem. One simplifying observation indicated, however, that the still-air buckling characteristics were not found to be significantly altered by a supersonic air stream. On the other hand, the panel-flutter characteristics of the shells were found to be strongly influenced by the viscous boundary layer, and initial geometric imperfections. Any analytical model must account for these significant features. The evolution of satisfactory design criteria, useful for estimating the aeroelastic stability and forced-response characteristics of thin-walled shell-type structures, promises to be a complex but interesting program.

REFERENCES

(1) Barr, G. W. and R. O. Stearman, "The Influence of a Supersonic Flow Field on the Elastic Stability of Thin Cylindrical Shells," *AIAA Structural Dynamic and Aeroelasticity Specialist Conference*, New Orleans, La., 16-17 April 1969.

(2) Stearman, R. O., "An Experimental Study on the Aeroelastic Stability of Thin Cylindrical Shells," *Abstracts of the 12th International Congress of Applied Mechanics*, Stanford University, August 1968.

(3) Stearman, R. O., "An Experimental Study on the Aeroelastic Stability of Thin Cylindrical Shells of the Lower Supersonic Mach Numbers," *Final Technical Report AFOSR 66-2828* and *ARL 67-0006*, December 1966.

(4) Barr, G. W. and R. O. Stearman, "Aeroelastic Stability Characteristics of Cylindrical Shells Considering Imperfections and Edge Constraint," *AIAA Paper Nr 68-285*, Presented at AIAA/ASME 9th Structures, Structural Dynamics and Materials Conference, April 1968.

(5) Weingarten, V. I., E. J. Morgan and P. Seide, "Final Report on Development of Design Criteria for Elastic Stability of Thin Shell Structures," *STL/TR-60-0000-19425*, Space Technology Laboratories, Inc., 31 December 1960.

(6) Fung, Y. C., "Some Recent Contributions to Panel Flutter Research," *AIAA Journal*, Vol I, pp. 898-909, 1963.

proof of a perfect code

DATA SCIENCES
LABORATORY
AFCRL

Of the 184 papers published by AFCRL scientists in the scientific literature during 1968, a paper by Dr. Vera S. Pless of the Data Sciences Laboratory was one of two selected to receive the Marcus D. O'Day Memorial Award. This award is made annually by AFCRL for an outstanding contribution to the scientific literature. Dr. Pless's paper, "On the Uniqueness of the Golay Codes," was published in the *Journal of Combinatorial Theory*, November 1968.

In her paper, Dr. Pless proves that the codes developed for one particular set of operational parameters, known as the Golay parameters, are uniquely perfect. The proofs take us deep into pure mathematics, with recondite conceptualizations that defy narrative description. But the results of this work have direct application to digital communication and pulse code modulation, the technique used by the Mariner spacecraft to transmit pictures of the Martian surface over tens of millions of miles with a transmission power of a few watts. The work falls within the general field of information theory, a field that had its origin in Claude Shannon's classic work in 1948. More specifically, the Pless study deals with error-correcting codes.

When binary digits are sent over channels that are noisy or imperfect, some check must be made at the receiving terminal on the accuracy of the transmission. For this purpose, a certain number of code digits are transmitted along with the information digits. This code automatically detects and corrects errors that may have occurred during transmission. Literally thousands of codes, all involving a kind of mathematical cryptography, have been developed for dealing with this problem.

Once a code is developed, however, there is no way of proving that it is the best possible code. Nor is there any way of comparing the relative efficiency of one good code against that of another good code. (An efficient code is one that can detect and correct a maximum number of errors using a minimum number of error-correcting—or parity—bits relative to information bits.) Few perfect codes have been found for any transmission situation; a major exception is a class of codes, known as the Golay codes, developed for transmission situations identified as the Golay parameters.

Investigators have long conjectured as to whether or not these codes are the only perfect ones for dealing with Golay parameters. Many have tried without success to find other perfect codes for dealing with these parameters. However, the Pless paper demonstrates that only the Golay codes are the perfect ones for dealing with the Golay parameters.

Dr. Vera S. Pless is a research mathematician in the Applied Mathematics Branch of the Data Sciences Laboratory, AFCRL. She is currently concerned chiefly with error-correcting codes, quadratic forms.

Dr. Pless received her Ph.B. in 1949 and her M.S. in 1952, both from the University of Chicago. In 1957 she earned her Ph.D. from Northwestern University. She is a member of both the American Mathematical Society and the Mathematical Association of America, and has published a number of articles in professional journals.

Dr. Vera S. Pless receives the annual Marcus D. O'Day Memorial Award from Colonel Dale J. Flinders, Commander of AFCRL. She was one of two AFCRL scientists to receive the award for outstanding scientific papers published during 1968. The award was granted to her for proving, by complex mathematical analysis, that certain error-correcting codes are uniquely perfect.

transducer-sensor generation gap

CAPT JOHN F. KANTAK
Directorate of Engineering Sciences, AFOSR

The difference in performance between our sophisticated electronic flight-control systems and the technologically outdated sensors that provide their input has created a generation gap. (1) Current control system capabilities are constrained by conventional sensor/transducer size, weight, frequency response, and temperature/shock sensitivities. Because these devices are forced to function at their maximum operational limits, they are a significant limitation to weapons-systems effectiveness. To alleviate this problem, Drs. L. K. Montieth, J. J. Wortman, and L. F. Ballard, at the Research Triangle Institute (RTI) in Durham, North Carolina, are investigating a class of organometallic compounds that may provide a technological impact equivalent to that of the transistor. Under the sponsorship of AFOSR, they are studying the electrical and structural properties of organometallic crystals, with the intention of creating solid-state sensors and transducers that are compatible with the size, performance, and power requirements of integrated circuits.

Organometallic compounds are a combination of organic molecules and metal atoms that can exist in liquid, powder, or crystalline form. Of the various possible organic and metal mixtures, the RTI research group is primarily interested in the subset of these compounds that have a major crystal axis (backbone) comprised of metal atoms. The interaction of the adjacent metal atoms along the backbone causes these organometallic crystals to perform like one-dimensional semiconductors. In addition to the semiconduction characteristic, these crystals are sensitive to both electromagnetic radiation and mechanical pressure. The electrical performance, exciting sensitivities, and high-device potential of these materials are sufficient motivation for the dynamic research currently under way at RTI.

Organometallic research started over a century ago with Frankland's discovery in 1849 of the first organometallic compound, diethylzinc. (2) During the following decades, chemists actively pursued the study of carbon-metal bonds or organometallic chemistry. Gradually the discipline wall between organic and inorganic chemistry was breached, and organometallic chemistry became one of the principal sources of growth technology for the field of organic chemistry. Among the major contributions from this early work are the expanded understanding of valence bonds(3) and the clarification of the role of orbital interactions.

However, rapid progress was inhibited because of the difficulty of synthesizing organometallic compounds, especially in crystal form. The metal atoms are oxygen sensitive and tend to decompose when subjected to the solvents generally used in crystal-growing processes. Advances were eventually made and various classes of crystals were grown that had the interesting electrical properties of a metal insulator. This characteristic was dominant because the metal atoms were isolated from each other by the nonconductive organic molecules. Thus, electronics interest lagged until the 1950s when the semiconductor properties of the transition-metal elements were discovered. The early semiconductor devices stressed the use of silicon and germanium and were quite effective in replacing the vacuum-tube technology with miniature equivalents. When it was found that the devices were temperature-sensitive, the search for other materials with comparable electronic properties was pressed. The organometallics appeared inviting because of their relatively high-temperature characteristics, but their organic insulating properties limited further interest until the early 1960s.

In 1964, Lewis and Nyholm(4) rekindled electronics aspirations when they discovered a synthesis technique for establishing the metal-metal bonds necessary for semiconduction in organometallic compounds. The mid-sixties thus

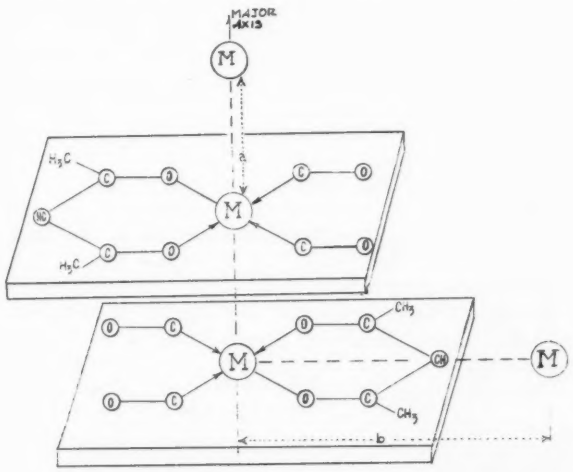

Figure 1. Organometallic crystal structure: a = 3.2 Å; b = 7.7 Å; M = metal atom.

witnessed an expansion of crystallization research. Growing organometallic crystals that have a metal-atom backbone is an extremely difficult process requiring a new method for almost every choice of metal and organic mixture; and even then only certain of the metals can be induced to form organometallic crystals. In general, a metal-backbone organometallic crystal can be described as having stacked planar molecules with metal atoms lining up along the major crystal axis (Figure 1). The metal atoms form metal-metal bonds by virtue of their close proximity (3.2Å), and the organic atoms attach themselves to the metals in a nonsymmetric manner by coordinate bonds. The chemical nature of the metal-organic bonds is governed

by the interaction of the organic Π-orbitals and the metal d shell orbitals to form a stable connection, while the metal-metal bonds are created by the interaction of the p and d shell orbitals of the adjacent metal atoms. These bond strengths can be rank-ordered as: metal-organic coordinate bonds and organic-organic coordinate or covalent bonds, with the metal-metal and intermolecular (lattice) bonds being comparable and weakest.

The chemical bonds and unpaired electrons give organometallic compounds novel physical properties. Included in the characteristics are: semiconduction along the metal-atom backbone, paramagnetism, and dichroism. The semiconductor properties are postulated to be the result of the interaction of the metal atoms which causes the conductivity along the metal-metal atom axis to be three orders of magnitude more than the conductivity normal to the axis (Figure 2). In effect, the crystal acts as an insulator in two dimensions and a semiconductor in the third.

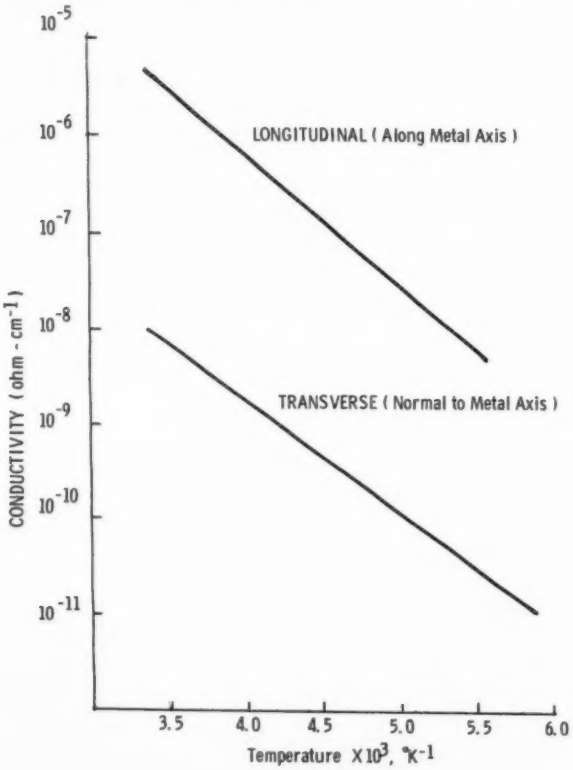

Figure 2. Conductivity at 10^3 Hertz.

Additionally, the magnetic moments (spin) of some of the metal electrons do not compensate each other, and their crystals have a permanent magnetic moment. This property is useful for studying crystalline electromagnetic fields and for high-frequency applications.

Another practical characteristic provided by some organometallic crystals is a novel sensitivity to electromagnetic radiation called dichroism. This phenomenon depends on the energy gap established by the crystal constituents, and is evidenced by novel light absorption/transmission properties. Crystals that have this property are sensitive to the polarization and wavelength of the incident radiation, as well as the angle of incidence relative to the major axis. This sensitivity becomes useful when it is transformed into a detectable current in the crystal. The amount of induced current in the crystal depends partly on the metal-atom electron structure; the elements thus vary the sensitivity of their organometallic products. Figure 3 indicates some of the more common organometallic metals, depicting copper as the metal providing the least sensitivity of the group, and osmium as the metal providing the most sensitivity.

This combination of very useful properties is the motivating force underlying the organometallic research of Drs. Montieth, Wortman, and Ballard. To exploit these material capabilities, they are attempting to achieve four fundamental objectives: (1) determine the influence of atomic spacing on the observed electrical properties; (2) determine the effects of reversible strain-induced changes in crystal molecular geometry; (3) define the precise causes for increased conductivity and radiation sensitivity with strain; and (4) identify and delineate material advantages and device constraints relative to stability, sensitivity, reproducibility, and lifetime. The scarcity of published information and almost nonexistent crystal-growing technology inhibits rapid progress toward these goals. The synthesis of organometallic crystals requires exceptionally pure materials, very stringent preparation procedures, and growth techniques which must be created as the research progresses.

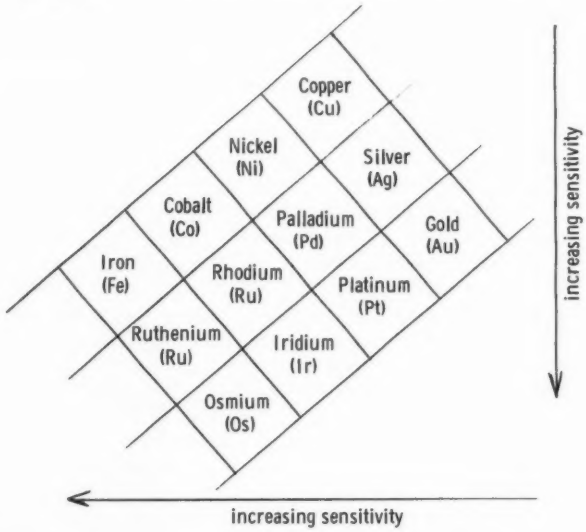

Figure 3. Metal radiation sensitivity for organometallic compounds.

The RTI research group has synthesized a wide variety of *metal-backbone* organometallic compounds during the last half decade. The elements they have used include: gold, cobalt, platinum, palladium, rhodium, irid-

ium, iron, tin, sulphur, mercury and nickel. (5,6) When the electrical properties of the organometallic compounds made from these elements were obtained and compared, the iridium (Ir*) and rhodium (Rh*) crystals exhibited a wide divergence in electrical conductivity (Figure 4). The five-

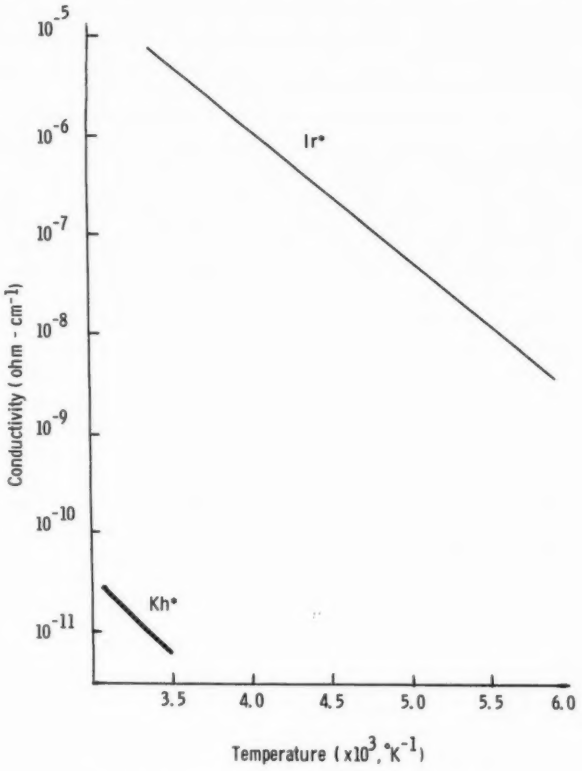

Figure 4. Longitudinal conductivity vs. temperature.

orders-of-magnitude difference was surprising since iridium and rhodium have very similar atomic structures and their organometallic crystals are identical. Anticipating a fundamental reason for the completely different performance, the RTI group is studying iridium and rhodium in depth.

To obtain useable samples of the iridium compound, dicarbonyl-2,4-dionatoiridium (Ir*), a suspension of tricarbonylchloroiridium and sodium bicarbonate in benzene (containing acetylacetone) was refluxed under a nitrogen atmosphere for five days. The reaction mixture was filtered and evaporated, and the product was purified by sublimation. Large (mm dimensions) single crystals were obtained by allowing the concentrated acetone solution to cool slowly to room temperature. In a similar manner, rhodium crystals, dicarbonylpentan-2,4-dionatorhodium (Rh*), were formed. This compound is obtained by refluxing a mixture of tetracarbonyl-μ-dichlorodirhodium, acetylacetone, and barium carbonate in petroleum ether. Again the nitrogen atmosphere was used to prevent oxygen damage during the crystallization process. Once the Ir* and Rh* crystals were obtained, the very real problem of affixing electrical contacts was addressed. The usual methods for placing contacts on semiconductor crystals cannot be used since these methods cause crystal damage and result in erroneous experimental data. To partially solve this problem, the electrodes are painted onto the organometallic crystals using a collodial silver dispersed in an organic solvent. This method minimizes crystal damage and is one of the most successful techniques employed to date.

The experimental data shown in Figure 4 clearly indicate a difference in electrical conductivity of as much as five orders of magnitude. One promising explanation for the difference has been hypothesized on the basis of the atomic structure of the metal atoms. The iridium atom-atom interaction is accomplished by the 5d orbitals, while the 4d orbitals provide the rhodium interaction. Since the spacing between the atoms of the two elements in their respective crystals is approximately the same (3.2Å), the larger iridium interaction apparently results from the extra molecular orbital overlap. This conclusion implies that mechanical forces could cause greater interactions between the metal-metal atoms and significantly improve the semiconduction mechanism.

To pursue this thought experimentally, two independent forms of mechanical force have been employed. The first force is a uniaxial mechanical stress that is impressed upon the major (metal-atom) crystal axis. This stress causes the metal atoms to be compressed, thereby increasing the orbital overlap and the metal-atom interaction. Obviously, since the crystal symmetry is changed, there could be off-axis crystal response which could be detrimental to the understanding of the force-induced performance. The second form of mechanical force, hydrostatic pressure, is used to investigate this possibility. Here the crystal symmetry is preserved. The hydrostatic force is applied to the entire crystal surface by immersing the crystal in an oil bath and applying pressure to the contained fluid. In this manner, the entire crystal lattice is subjected to mechanical forces, and off-axis response is not a consideration. In both methods, the electrical resistance of the crystal versus the magnitude of the applied force is recorded. To interpret the significance of the data, a gauge factor (G.F.) is computed for each type of force.

The gauge factor for the uniaxial stress is computed by dividing the quotient of the change in crystal resistance and the ambient resistance by the quotient of the change in crystal length and the normal length ($G.F. = \frac{\Delta R/R}{\Delta L/L}$). For the case of hydrostatic pressure, the measure used is the quotient of the change in crystal resistance and ambient resistance divided by the quotient of the change in pressure on the crystal and the oil pressure on the crystal that results from immersion only, ($\frac{\Delta R/R}{\Delta P/P}$).

Gauge factors are used to define a figure of merit for the organometallic compounds relative to other known sensor materials. For instance, Ir* has a G.F. of 135 compared to a G.F. of 100 for silicon and a G.F. of 3 for standard metals. For hydrostatic pressures, Rh* has a $\frac{\Delta R/R}{\Delta P/P}$ of 5 compared to zero for silicon and germanium. This

sensitivity, exceeding that of commonly used sensor materials, coupled with the very small size, excites device-oriented imaginations. Typical data curves for Ir* and Rh* are presented in Figures 5 and 6.(7) The curves display a definite decrease in electrical resistance (increasing conductivity) with increasing mechanical force. These data support the orbital-overlap theory of the RTI group, and represent a significant step forward in metal-backbone organometallic sensor research. Investigations are continuing in an effort to define the mechanisms responsible for the electrical performance and to achieve the theoretically predicted six-orders-of-magnitude increase. Further research should define the electron-transport mechanism that allows these materials to perform as semiconductors, and explicitly define the intermolecular actions that provide the radiation sensitivity.

Crystals of Ir* and Rh* are selectively sensitive to incident electromagnetic radiation, i.e., they exhibit dichroism. The crystals of Ir* are bronze and those of Rh* are green by reflected light; but they transmit blue and red, respectively. The crystal response depends upon the wavelength, polarization, and angle of incidence of the impinging radiation. Crystal response is optimized if the illuminating energy is perpendicular to, and polarized along, the metal-atom backbone. Typical infrared absorption data for Ir* and Rh* are shown in Figure 7. The percent of radiation absorbed is plotted versus the radiation wavelength and over the near-infrared atmospheric transmission windows. The high level of absorption displayed by Rh* in the five-micron "window" has significant implications for radiation sensor applications. Additionally, the fact that Rh* is sensitive to mechanical forces implies that such a sensor might be tuned by applying external pressures. These characteristics, radiation and pressure sensitivity, of metal-backbone organometallics are sufficient motivation for dynamic and widespread research activities.

The international significance of research on organometallic materials can be deduced from a survey of the open literature. Scientists in many countries are involved in the field; but the major efforts are found in the U.S., the U.K. and the U.S.S.R. Figure 8 indicates the coincidence of national efforts relative to the basic metals used to create organometallic compounds.(8) Although different individual elements are emphasized, and a large number have been studied, the listed elements are those most often reported in the literature. For example, during the 1960s, the Russians stressed studies of organosilicon, organogermanium, copper, and ferrocenes. These materials exhibit the previously described organometallic metal-backbone characteristics, but to a lesser degree than crystals created from other elements like platinum, palladium, or iridium which have had the attention of a good portion of the research efforts in the U.S. and U.K. It should be noted that all three of the major national efforts are studying

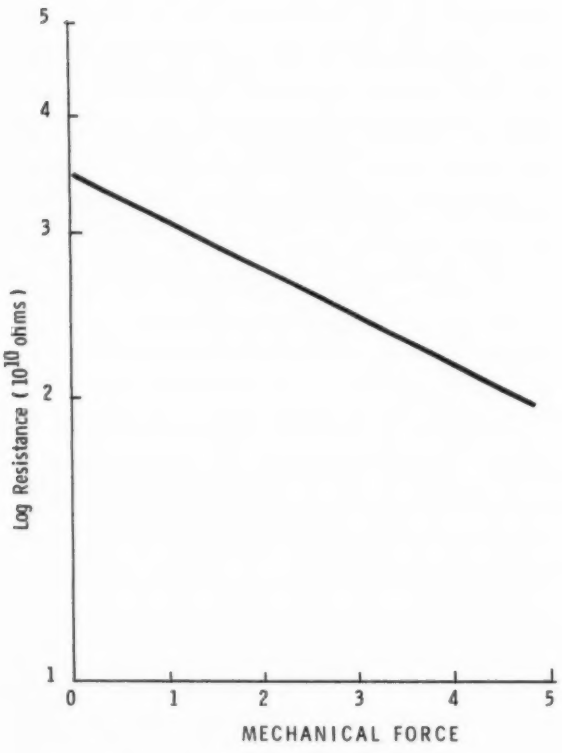

Figure 5. Ir* response to uniaxial strain.

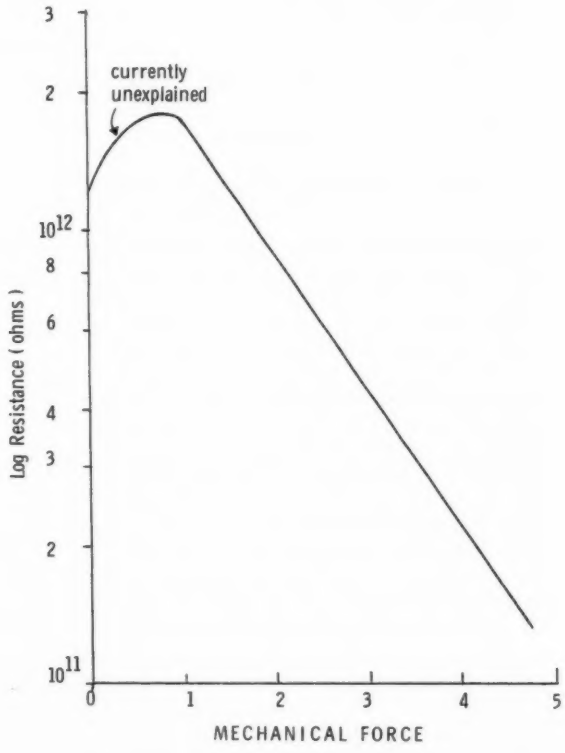

Figure 6. Rh* response to hydrostatic pressure.

general derivatives using these elements with particular organic groups to form compounds such as bromides, polysilanes, imines, amines and salts. The motivation for investigating a wide variety of compounds is based on the need to find exploitable device characteristics. The elements included in Figure 8 comprise less than half of the elements successfully synthesized into organometallic compounds. The unlisted elements are receiving minimal attention because of the greater device potential or research value exhibited by the listed elements.

Relevant applications that are in being or forecast for organometallic materials are presented in Figure 9. The list was compiled from the open literature and no attempt was made to determine classified objectives. Electronics applications that are ready for technological development are determined by the demonstrated capabilities of organometallics as: dielectric materials; electrically resistive mediums for attenuators; and electrical insulators. Similar applications outside the electronics field include: propellant additives; anticorrosion materials; and chemical catalysts. Although not widely employed in these problem areas, organometallics have a proven ability that could be technologically fruitful. There are some very difficult problems to be solved before superconduction and lasing will be achieved with these materials; but investigations are currently under way. Also being studied are the semiconductor, sensor, and transducer applications where the problems to be solved are less stringent and the device potential is extremely high. The general applications are chemical in nature. Insensitivity of the materials to high temperatures is provided by the organic constituents, a property that has both military and commercial implications.

In summary, the AFOSR-sponsored research of Drs. Montieth, Wortman, and Ballard is contributing significant scientific knowledge to the field of organometallic chemistry and solid-state electronics. By explaining and exploiting the fundamental mechanisms causing the pressure and radiation sensitivities of metal-backbone organometallic compounds, they are closing the transducer-sensor genera-

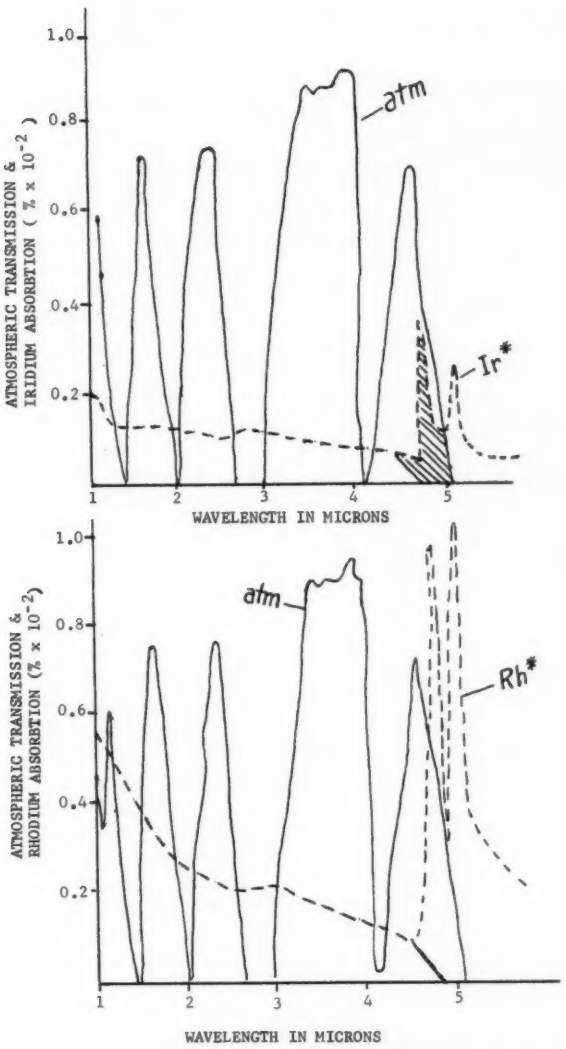

Figure 7. Radiation sensitivity.

ELEMENTS	USA	USSR	UK
silicon	X	X	X
germanium	X	X	X
platinum	X	X	X
iron	X	X	X
iridium	X	X	X
rhodium	X	X	X
gold	X		X
cobalt	X	X	X
copper	X	X	X
nickel	X	X	X
palladium	X		X
zinc	X		X
sodium	X	X	
potassium	X	X	
tin	X		X

NOTE: ELEMENTS' INCLUSION REQUIRED AT LEAST TWO-NATION INTEREST

Figure 8. Elements synthesized into organometallic compounds.

ELECTRONICS APPLICATIONS	USA	USSR
rf attenuators	X	X
dielectric material	X	X
electrical insulator	X	X
semiconductor	X	X
superconductor	X	
sensor	X	
transducer	X	X
laser material		X
GENERAL APPLICATIONS		
high-temperature hydraulic fluid	X	
high-temperature resin	X	X
high-temperature ablative	X	X
catalyst	X	
propellant additive	X	X
bond strengthener	X	
anticorrosion additive	X	X

Figure 9. Applications for organometallic compounds.

tion gap. The applications potential of organometallics *should* have an explosive impact on the technology of the next decade, and significantly improve the capabilities of the USAF.

REFERENCES

(1) Neswald, R. G., "Transducers: On to Solid State," *Space/Aeronautics,* Feb. 1969, pp. 63-72.

(2) Eisch, J. J., *The Chemistry of Organometallic Compounds,* New York, N.Y.: Macmillan Co., 1967.

(3) Matuszko, A. J., "Organometallic Chemistry," *AFOSR Research,* AD659366, July 1967, pp. 165-169.

(4) Lewis, J. and R. S. Nyholm, *Science Progress,* Vol. 52, 1964, p. 557.

(5) Montieth, L. K. et al, "Synthesis and Characterization of Intermetallic Polymers," *AFAL Technical Report TR-66-389,* December 1966.

(6) Ballard, L. F., "Electronic Conduction in Organometallic Complexes of Transition Metals," *Research Triangle Institute Technical Note No. 19,* (MS Thesis - Duke University), December 1966.

(7) Montieth, L. K. et al, "Synthesis and Characterization of Intermetallic Polymers," *AFAL Tech. Report TR-68-18,* Jan. 1968.

(8) Compiled from various volumes of *Aerospace Technology,* Division Press; various volumes of the *Journal of Organometallic Chemistry,* Elsevier Pub. Co., the Netherlands; *Chemistry of Organometallic Compounds,* ATD Report 66-47; and *Organosilicon and Organometallic Compounds,* AID Report 62-196.

CLOUD PATTERNS ON A SUMMER DAY

METEOROLOGY LABORATORY, AFCRL

Take two benign cumulus clouds of the type that drift across the sky to lend interest and variety to a bright summer day. Observe them for a while. You may see that both are born and reach maturity in less than 10 minutes. You may also see that 1 begins to decrease in size and that soon, about 20 minutes from birth, it has disappeared. The other continues to grow, reaching a diameter of over a mile and may persist for an hour and a half. It may even, although rarely, produce a rain shower. Why did one quickly dissipate, while the other continued to grow into a sizable system?

Actually, we can't say. The meteorologist knows much more about the brother of our two clouds, the giant thunderstorms with their turbulence, hail and wind. He can tell you with some confidence that "thunderstorms are likely to develop in the afternoon"; but it is only with faltering assurance that he will predict the intermittent light rain showers that our summer cumulus might produce.

Now suppose, assuming an average day with a normal population of cumulus clouds in the sky, that we pick a cloud at random and seed it with silver iodide. Chances are that our seeded cloud would follow a growth and dissipation pattern that would be indistinguishable from that of similar neighboring clouds. This isn't to say

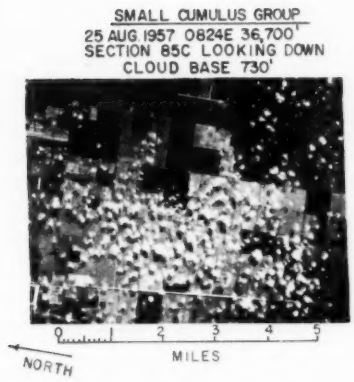

Figure 1. If one looks closely at this population of cumulus clouds, one can discern a row structure. The patterns assumed by cumulus-cloud populations can be studied to determine the nature of convection currents over various land areas.

that on other days, given certain conditions of humidity, temperature and so on, the seeding might not produce mushrooming cloud growth. But, in general, in view of the large normal variability that is known to prevail in the life cycles of convective clouds, the effects of seeding would be difficult to detect unless observations were made in a very meticulous manner.

Cloud modification is one of the considerations behind AFCRL's study of cumulus-cloud populations, conducted by Mr. Vernon G. Plank of AFCRL's Meteorology Laboratory. The patterns of cumulus populations are the visual tracers of the regions of updraft motion within a general convective layer, showing the transport of heat and water vapor upward to the cloud-base level. One recent study of cumulus populations involved a U-2 aircraft flying at 66,000 feet and taking time-lapse photographs for several hours. When projected, the photographs made vividly apparent the horizon-to-horizon changes and motions of the cloud populations.

The time-lapse photography revealed many features of cumulus-cloud populations that were obscured in real-time observations. When cumulus clouds formed in long rows, as they often do, it was shown that they could appear in fully developed form along a 20-mile line within 4 to 8 minutes. The organized circulations responsible for the rows were obviously present in the subcloud layer prior to the condensation of the clouds. Also, the clouds that formed in the patterned cloud row were found to persist longer than clouds in a nonpatterned population.

The time-lapse pictures were especially valuable in providing information on the persistence of clouds as a function of initial size. It was found that the variability of persistence in clouds of the same initial size was extremely large. For no precisely defined reason (but many speculative ones), some clouds dissipate quickly, while others grow to relatively large size. It is this variability that makes it difficult for the cloud physicist to assess the effects of seeding.

Mr. Vernon G. Plank is a research physicist with the Convective Cloud Physics Branch, Meteorology Laboratory, AFCRL. He has been at AFCRL since 1951, conducting research in the fields of radar meteorology and cloud physics, with special emphasis on the radar characteristics of clouds, spurious echoes on radar, the refractive index structure of cloudy regions, and the effects of clouds on the radio guidance of space vehicles. Prior to that time, from 1947 to 1951, he was a meteorologist with the U.S. Navy Electronics Laboratory in San Diego, California. There he conducted research on special meteorological instrumentation and on the meteorology of radio-wave propagation.

In 1949, Mr. Plank received his A.B. in Meteorology from the University of California at Los Angeles, and in 1954 his M.S. in Meteorology from the Massachusetts Institute of Technology. He is a member of the American Meteorological Society, and the American Geophysical Union, and is also an honorary member of the Research Society of America. He has a number of published scientific articles to his credit.

Mr. Vernon G. Plank, AFCRL meteorologist, examines a plot showing the growth of a cumulus cloud. He is one of the nation's authorities on cumulus-cloud populations.

DR. W. G. BRAUN
Plasma Physics Research Laboratory, ARL

argon plasma spectroscopy

The value of spectroscopic methods for plasmadiagnostics has been pointed out by many authors, but the correct and accurate interpretation of the measurements depends on the establishment of a reliable system of atomic parameters. Measurements with radiation sources operated under conditions which permit the application of certain theoretical relations provide atomic constants such as energy levels, transition probabilities, and line-broadening parameters. Only in very few spectroscopic sources do conditions prevail which allow conclusions based on the validity of the Boltzmann distribution formula or Kirchhoff's law. The ideal source for quantitative spectroscopic investigations would be a plasma in local thermodynamic equilibrium (LTE) but, with laboratory-produced plasmas, deviations from LTE must be tolerated, assessed, and allowed for in the evaluation of the data, if possible.

Atomic parameters of argon have been obtained from measurements with electrical-arc discharges which have been evaluated with the assumption of LTE. Olsen (1) used a free-burning arc between a pointed tungsten cathode and a flat copper anode and, in a detailed study, found incompatibilities in the results which he traced to deviations from LTE in his arc. The complex, intriguing problem invited another investigation of the argon arc discharge in the Plasma Physics Research Laboratory. A vortex stabilized arc and a free-burning arc as used by Olsen (2) were probed spectroscopically in emission and absorption by the tracking-mirror method (Figure 1).

The central intensity of the arc was reflected by a concave mirror through the discharge, and served as the probing intensity I_o for the determination of the transmission factor $T(x)$ as a function of the distance x between the probing ray and the axis of the arc. The variation of x was achieved by slow rotation of the flat scanning mirror and by coordinated travel along a circular path of the concave tracking mirror while the source, the condenser lens, and the monochromator remained fixed. In this scanning system, the reciprocal of the radius of the tracking path equals the mean of the reciprocals of the distance between the vortex of the concave mirror and the pivot of the scanning mirror and the distance from tracking mirror to the source; the latter distance equals the radius of curvature of the spherical tracking mirror. The analogy of this relation with the imaging formula of a spherical mirror with a radius of curvature equal to the radius of the tracking path is obvious.

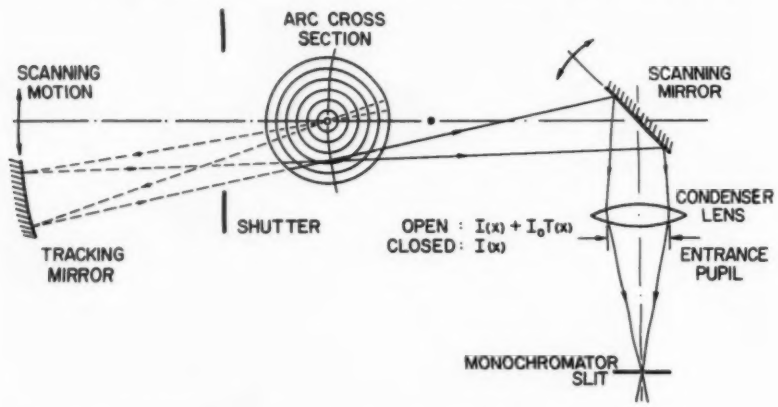

Figure 1. Optics for the measurements of the coefficients of absorption and emission in a rotationally symmetric source.

The arc displays rotational symmetry, but the cross section changes significantly from cathode to anode. In order to minimize the spatial averaging in the measurements, a rectangular entrance pupil of low height parallel to the arc axis was used. This resulted in a small angular aperture. Of equal importance, the entrance slit of the monochromator, which is parallel to the axis, was limited in height by an additional horizontal slit in place of the usual Hartmann slide so that the slit image formed in the midplane of the source by the condenser lens measured only 50 by 500 μm. This slit image scanned the arc halfway between the cathode and anode. Lateral transmission factor profiles were determined from alternating intensity measurements; one made with the probing intensity, the other with the mirror path blocked by a chopper blade. The probing intensity was obtained in the marginal positions of each scan when the probing ray bypassed the arc. Among several tests which were carried out to insure the validity of the transmission-factor measurements, the following is noteworthy: deflection of the probing ray by refraction in the source which would cause an error in the measurements was examined by vignetting the pupil on the tracking mirror (Figure 2). The entrance pupil of the monochromator is the image of the grating mask in the condenser lens formed by the entrance slit; a similar rectangular pupil on the tracking mirror collects the probing intensity. During a scan this pupil does not move relative to the mirror unless the probing ray is deflected by the source. Covering part of the pupil on the tracking mirror by a mask cut parallel to the arc axis reduces the probing intensity. If refraction occurred in the source, the angle of deflection of the

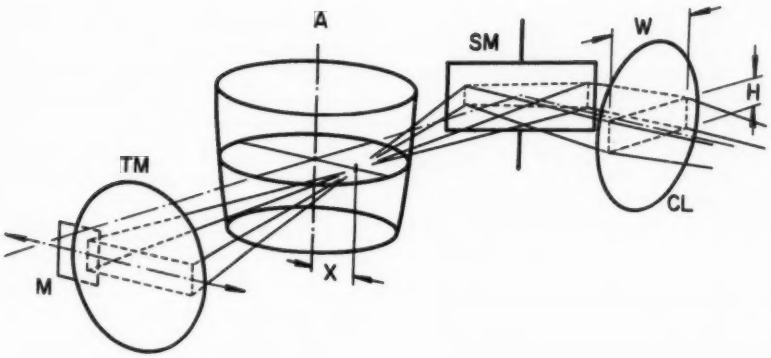

Figure 2. Passage of probing rays. CL: condenser lens; W and H: width and height of entrance pupil; SM: scanning mirror; A: axis of arc; X: momentary scanning position; TM: concave tracking mirror; M: mask for test.

probing ray would change during a scan, and transmission profiles obtained with the mask in place would exhibit asymmetry with respect to the central position because a deflection caused by the inhomogeneous but symmetric source would change direction when the scan passes the center. If refraction moves the pupil away from the masked portion of the mirror and increases the probing intensity on one side, it would move the pupil into the mask and decrease the intensity on the other side. Even in the vicinity of a strong absorption line, refraction in the source could not be detected by this method. Consequently, during a scan, the probing intensity is always obtained from rays which pass through the axis of the arc, and I_o is constant as is assumed in the evaluation of the interlaced intensity profiles.

The logarithm of the transmission factor and the local absorption coefficient in a rotationally symmetric source are linked by an Abel-type integral equation which has been solved by a numerical technique developed by Birkeland and Oss. (3) The result of an experiment in the vicinity of the Argon I line at 7637 Å is presented in Figure 3. The height of the surface drawn by a computer program represents the absorption coefficient as a function of wavelength and the distance from the center of the arc. True values of the absorption coefficient can not be expected in those zones of the profile where the spectral resolution of the monochromator used approaches the width of the absorption line, nor in those wavelength regions where the transmission factor approaches unity, i.e., where the arc plasma is optically thin. Aside from the variations in width and the shift of the absorption line in the core of the arc, the surface discloses a narrow absorption ring at a radius of about 5.5 mm. Simultaneously obtained profiles of the emission coefficient vanish for radii greater than 3.5 mm which indicates an overpopulation of atoms in the lower, metastable state of the observed transition in the ring. Similar rings were obtained at the wavelengths of other transitions to the same level pointing to a sheath of metastable atoms around the arc. This means a deviation from LTE, i.e., the distance a particle travels between equilibrating collisions spans too large a change in electron density and temperature despite the high pressure in the discharge. But allowance for the measured self-absorption in the evaluation of the intensity profiles restores the validity of the transition probabilities obtained with this arc. An absorbing sheath which is caused by the ultraviolet resonance radiation emitted by the core of the arc has been detected also. This again is evidence that the mean free path of the photons is larger than the core of the arc but, in principle, this is com-

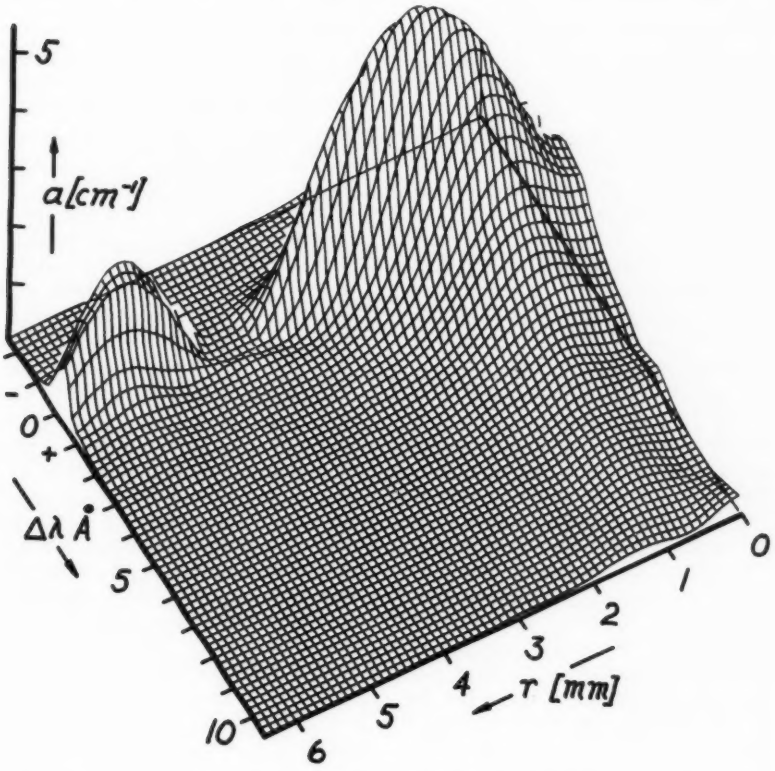

Figure 3. Absorption coefficient a(λ,r) in the cross section of an argon arc at 7637Å and at a pressure of 2 atmospheres.

patible with the concept of LTE.

The examples presented demonstrate the value of the experimental determination of the absorption profiles in spectroscopic measurements with arc discharges.

Work in progress concerns the collection of more experimental data on which a quantitative assessment of deviations from local thermodynamic equilibrium in arc plasmas can be based.

REFERENCES

(1) Olsen, H. N. et al, "Determination of Departures from Local Thermodynamic Equilibrium in Arc Plasmas," *ARL Report 67-0060*, March 1967.

(2) Olsen, H. N., "The Electric Arc as a Light Source for Quantitative Spectroscopy," *J. Quant. Spectros. Radiat. Transfer, 3*, 305 (1963).

(3) Birkeland, J. W. and J. P. Oss, "Spatial Resolution of the Volume Emission Coefficient in Strongly Self-Absorbing Sources of Cylindrical Symmetry," *J. Applied Optics, 7*, 1635 (1968).

Dr. W. G. Braun received the M. S. Degree in Applied Physics from the Technical University in Vienna, Austria and, in 1957, the Dr.-Ing. Degree in Applied Physics from the Technical University in Darmstadt, Germany. When he joined ARL's Plasma Physics Research Laboratory in 1958, he concentrated on his original field of specialization, the physics of electrical discharges through gases. Focussing his interest on diagnostic techniques, he started experimental work in high-speed photographic techniques and in spectroscopic methods, and pioneered the utilization of automated data acquisition with physical experiments to achieve extreme accuracy of the measurements. He currently leads the research effort in high-energy density plasma diagnostics at ARL.

Dr. Braun has received an Air Force Award for Sustained Superior Services. He was a member of the National Research Council of the National Academy of Sciences in 1960, and a member of the NASA Research Advisory Committee on Fluid Mechanics for two fiscal terms. He is an active member of the Institute of Electrical and Electronic Engineers and of the American Physical Society, Division of Plasma Physics, and has several articles and two patents (as coinventor) to his credit.

some recent developments in strong interaction physics

DR. ERICH WEIGOLD
Directorate of
Physical Sciences
AFOSR

Reactions of the type a + b → c + d are called two-particle reactions, and their study is an important topic in hadron (strong-interaction) physics. Any such reaction can be described by three kinematical invariants, the so-called "Mandelstam variables" s, t, and u, where s is the square of the center of mass energy, t is the square of the momentum transfer between particles a and c (or b and d), and u is the square of the momentum transfer between particles a and d (or c and b). These three variables are not independent, since their sum is equal to the sum of the squares of all the four masses. We can, therefore, describe the two-particle reaction with a scattering amplitude, A(s,t), which is a function of only two parameters. The third parameter, u, becomes important when we consider the crossing symmetric reaction—that is, if we replace an incoming particle of momentum, p, with an outgoing antiparticle of momentum, -p, and an outgoing particle by an incoming antiparticle of opposite momentum. In this case, s exchanges roles with either u or t.

Although there is at present no complete theory for the calculation of the scattering amplitude, A, of one hadron by another, various models have been developed in order to deal with this situation. The Regge-pole method, which was developed from analogy with potential scattering, remains the most successful attempt to understand the scattering of particles at high energies. When two hadrons interact at high energies, they may exchange a number of particles. In the t-channel, these exchanged particles appear as free particles which can transfer not only momentum but also various intrinsic quantum numbers. Exchanged particles with the same intrinsic quantum numbers, but different angular momentums, are said to be members of the same Regge family. In terms of a continuous angular momentum variable, a plot of the masses of these particles versus angular momentums gives rise to the so-called Regge trajectory.

The Regge-pole model leads to an asymptotic formula for the scattering amplitude, A (s,t), at large energy, s, and fixed momentum transfer, t:

$$A(s,t) \cong B(t)\ \frac{s^{\alpha(t)}\left[e^{-i\pi\alpha(t)} \pm 1\right]}{\sin\pi\alpha(t)}$$

where $\alpha(t)$ is the Regge trajectory and the coefficient B(t) is known as the residue. The actual masses of particles exchanged in the t-channel are the values of $\sqrt{t}$ at integer or half-integer values of the angular momentum. We can see that the Regge model leads to a very important connection between the asymptotic behavior in the s-channel and the t-channel resonances.

During the past few years, several significant developments have occurred. First of all, S. Mandelstam, (1) who is supported by AFOSR, has suggested that Regge trajectories could have completely different shapes from that suggested by potential scattering where, in a two-body problem, resonances with large values of angular momentum are not allowed because of the centrifugal barrier. He pointed out that the essential many-body nature of elementary-particle physics should give rise to ever-increasing Regge trajectories, and then developed a dynamical scheme based on such indefinitely rising trajectories. This suggestion has been supported by experiments which do seem to indicate that the trajectories are linear, i.e., that $\alpha(t) = at+b$.

Other work showed that, in order to satisfy the relativistic invariance and analyticity of the scattering amplitude, A, a great many complicated conditions (called conspiracies and evasions), as well as new daughter trajectories, had to be introduced. In brief, all these complications led to extensive changes in the original Regge-pole ideas.

Another significant recent development was the recognition of duality between the low-energy resonance production picture and the high-energy Regge-pole picture. This important discovery, that the Regge-pole picture is useful not only in the asymptotic energy region but also in the low-energy region, resulted from an interesting new application of the Regge approach known as finite energy sum rules. These sum rules relate the low-energy resonance data in a given channel to the leading Regge trajectories. R. Dolen, D. Horn, and C. Schmid (2) were the first to point out that resonances and Regge poles are, in an average sense, the same things said in two different ways.

What was needed now was a closed mathematical expression summarizing the new type of Reggeology, which had almost completely lost its original potential-scattering background. This closed expression for two-particle reactions was provided by the Veneziano (3) formula which, for spinless particles, is:

$$A(s,t,u) = \text{Const}\,[B(1-\alpha(s), 1-\alpha(t)) + B(1-\alpha(s), 1-\alpha(u)) + B(1-\alpha(t), 1-\alpha(u))]$$

where B is the Euler beta function.

It is easy to show that this formula has the required analyticity, contains the duality principle, has Regge asymptotic behavior, and satisfies all the finite energy sum rules. In addition, the formula is explicitly crossing invariant so that the analytic and asymptotic properties of the scattering amplitude are the same in all three channels.

The Veneziano representation was quickly generalized by K. Bardakci and H. Ruegg, (4) supported in part by AFOSR, to the case where any number of particles may occur in the final state of the reaction. Further, some very interesting results have arisen from recent attempts to include internal symmetry and spin in the Veneziano model. In particular, Mandelstam (5) used a relativistic quark* model to develop a dynamical scheme based on the Veneziano formalism. Although the system contains no physical quarks, and therefore does not require their existence, he found the spectrum of particles to be the same as that predicted by the nonrelativistic quark model.

In the meantime, H. Harari (6) and J. Rosner, (7) both supported by AFOSR, independently proposed a simple type of diagram, based on the quark model, which exhibits the duality principle in a striking way, and which can be used to determine the presence of "exotic" particle resonances. The diagrams avoided the underlying redundancy in the usual Regge descriptions and enabled the easy reproduction of a large number of known predictions of the duality picture, as well as an even greater number of new predictions.

More recently still, K. Bardakci and M. B. Halpern, (8) again supported in part by AFOSR, have generalized these ideas and found a completely factorized model with spin and internal symmetry to describe the dynamics of strong interactions. This model has the required analyticity, realizes precisely the duality diagrams of Harari and Rosner, contains Mandelstam's solution, and does not appear to depend on any underlying quark parameters.

At present most of the theorists working on the representation are attempting to make the theory unitary, since probability must be conserved. If this can be achieved, a real understanding of many of the problems of strong interaction physics may be possible. Since, in the opinion of this author, a conceptual breakthrough necessarily precedes a significant technological breakthrough, it is of obvious interest to the Air Force to foster research aimed at understanding the fundamental nature of matter and energy.

A quark is a hypothetical particle with fractional charge considered to be the building block of the known fundamental particles.

REFERENCES

(1) Mandelstam, S., "Dynamics Based on Rising Regge Trajectories," *Phys. Rev. 166*, 1539-1552, 1968.

(2) Dolen, R., D. Horn and C. Schmid, "Finite-Energy Sum Rules and Their Application to π N Charge Exchange," *Phys. Rev. 166*, 1768-1781, 1968.

(3) Veneziano, G., "Construction of a Crossing-Symmetric, Regge-Behaved Amplitude for Linearly Rising Trajectories," *Nuovo Cimento 57A*, 190-197, 1968.

(4) Bardakci, K. and H. Ruegg, "Reggeized Resonance Model for Arbitrary Production Processes," University of California, Berkeley, Preprint, 1969.

(5) Mandelstam, S., "A Relativistic Quark Model Based on the Veneziano Representation, I. Meson Trajectories," University of California, Berkeley, Preprint, 1969.

(6) Harari, H., "Duality Diagrams," *Phys. Rev. Letters 22*, No. 11, 562-565, March 1969.

(7) Rosner, J., "Graphical Form of Duality," *Phys. Rev. Letters 22*, No. 13, 689-692, March 1969.

(8) Bardakci, K. and M. B. Halpern, "A Possible Born Term for the Hadron Bootstrap," University of California, Berkeley, Preprint, 1969.

PERCEPTION VS. IMAGERY

DR. GLEN FINCH
Directorate of Life Sciences
AFOSR

Research on perception is increasingly emphasizing the characteristics of the human subject rather than those of the physical stimulus. It is well established that patterns are recognized and interpreted largely on the basis of the past experience of the human observer. Research on sensory adaptation, depth perception, and auditory discrimination emphasizes the important contribution to the perceiving process of what is inside the perceiver, including his expectations, his past experience, and his readiness to form a mental facsimile of the external object from minimal cues.

Research findings suggest the possibility that the observer also brings expectancies concerning the sensory channel through which external stimuli may enter the system. However, just as an observer who is anticipating a three-dimensional object may make certain characteristic errors in his perception of a two-dimensional figure, so an observer who is anticipating a mental image may fail to recognize that an external stimulus was also present. An observer who is anticipating a stimulus may mistake his image for the real thing. Some psychologists have asserted that the channel through which a stimulus enters is equipped with a mechanism which identifies the channel. However, there is convincing evidence that, with weak or ambiguous signals, this is not the case, and the channel is not always correctly identified. Normal people may make errors in locating the source of an experience: they may miss the signal when it is really present, or they may imagine that a signal is present when it really is not.

As these errors are potentially serious for a pilot who must frequently make important, immediate decisions in the presence of minimal or ambiguous information, these errors are being systematically investigated by AFOSR-supported research. The effects of different characteristics of the stimulus, differential information about the stimulus, and different types of ongoing tasks which may distract the subject's attention from the stimulus are all being studied. In addition, certain characteristic individual differences are being explored to determine how specific individuals react to these situations and to determine if drowsiness has a differential effect on different persons.

Under AFOSR sponsorship, Dr. Sydney J. Segal of the City University of New York has conducted a series of experiments bearing on these problems. In one experiment, the subjects looking at a dark screen through a small tunnel strapped to the head imaged a series of objects and, at the conclusion of the procedure, (1) they were informed that dim slides had been projected on the screen, and (2) they were asked to report from memory which of the images were, and which were not, accompanied by slides. Sensitivity was very poor in this task and subjective bias was also low. There was a fairly even distribution of misses and false alarms. In a second condition, the subjects were told in advance that slides might be projected and that they would be asked after each image if a slide accompanied it. Sensitivity was greatly improved and bias (i.e., imbalance between number of failures to detect the stimulus and the number of false alarms) was also increased. In another condition, the subjects projected the slides themselves. This improved sensitivity and decreased bias slightly. Finally, in a straight discrimination task where the subjects were required only to report on the presence or absence of slides and no imagery was obtained, sensitivity was maximized and bias reduced. In another variation of this procedure, intensity of the stimuli was reduced and sensitivity declined, while bias increased. When the stimulus onset was varied, sensitivity was greatest with immediate onset.

In conclusion, there seems to be no unmistakable subjective distinction between reality (external input) and illusion (internally generated events). Experienced pilots are aware of the fact that they are subject at times to visual illusions. Since pilots must rely to a considerable degree upon visual cues, it is important that they be able to distinguish between perceived and imaged objects, and that they be aware of sources of error in their functioning and decision strategies. Male subjects tend to avoid the false alarm–they are reluctant to report something that may not be there. This may lead to raised criteria for detecting true stimuli and carry with it the likelihood of missing more stimuli. Realizing that false alarms and misses will occur, pilots should adopt the detection strategy most appropriate to the situation in which they find themselves. If there is no penalty for false alarms, the strategy should emphasize reduction of misses by lowering the criteria of acceptable reports of stimulus presence. If the penalty for false alarms is great, these criteria should be more stringent.

REFERENCES

(1) Segal, S. J., "The Perky Effect: Changes in Reality Judgments with Changing Methods of Inquiry," *Psychon. Sci., 12,* 393-394, 1968.
(2) Segal, S. J., "The Perky Effect Revisited: Paradoxical Threshold or Signal-Detection Error," *Percept. Mot. Skills,* 1969, (in press).
(3) Segal, S. J. and V. Fusella, "Effects of Imaging on Signal-to-Noise Ratio, with Varying Signal Conditions," *Brit. J. Psychol.,* 1969, (in press).

LT COL ROBERT B. KALISCH *
Directorate of
Engineering Sciences
AFOSR

A LITTLE BIT OF DATA

A critical problem caused by the current trend of automation and computer computation is that of high-density data storage. The Air Force is sensitive to the need to reduce the physical size of digital memories and at the same time increase the data capacity. Many new and proposed data systems are affected by the conflicting requirements for physical space, computation capability, and memory storage.

This motivation has given rise to a number of creative research efforts, with several approaches to data storage showing promise. Most studies have concentrated on a technique for changing the state of a physically small region and a technique for determining the state of some stored bit in the material. These problems have suggested the use of laser beams and electron beams to "read" and "write." Such beams can be focussed to extremely small dimensions.

The electron beam has the advantage of ease of deflection, but this quality is counterbalanced by the vacuum requirements for an electron-beam system. Significant work in scanning electron-beam microscopy has advanced the state-of-the-art to a point at which data-storage techniques appear possible. Electron-beam storage devices have been studied and show considerable promise.(1)

In laser data-storage techniques, important results have been achieved by Professor D. I. Tchernev of the University of Texas, with Joint Services Electronics Program support from AFOSR. Professor Tchernev's work has been primarily with thin films. In general terms, the technique is to create a thin film with uniform magnetic properties, which are altered over small areas by a writing laser. Hence, binary data is stored in the thin film. The read-out is optically possible because the magnetic state of the thin film alters the optical transmission of the film. A laser is also used for read-out, but operates at a lower power level.

Several questions arise concerning the thin-film approach. For example, what thin film will have the desired properties? Ideally, the material should be easily deposited, have good mechanical properties, experience magnetization change (Curie temperature) at convenient temperatures, and cause a large Faraday rotation difference in the two magnetic states. This technique is dependent upon rotation of the plane of polarization of light as it passes through the thin film. Most magnetic materials have very low transmission coefficients for visible light. As a result, the film must be very thin—actually, less than a thousand angstroms. This problem, coupled with the need for thermophysical properties compatible with laser-beam heating, has led to the study of various materials.

One material under consideration has been manganese bismuth (MnBi), vacuum deposited sequentially on a freshly cleaved mica substrate. The mica substrate is important in that it causes the MnBi crystal growth along the easy axis of magnetization. Such films require a nominal 4000 Oe field to become saturated, while an oppositely directed field of 1500 Oe will reduce the magnetization to zero. For a thickness of 700 angstroms, the optical transmission was 3 percent with a Faraday rotation of $\pm 1.65^\circ$.(2)

If a laser is used to do the writing, the manganese bismuth is heated to a temperature above the Curie point (360°C), but below the destruction temperature (446°C). This narrow temperature range for writing is, of course, a significant limitation of manganese bismuth.(3) A much larger temperature differential between the Curie point and the destruction point would be desirable.

Other materials studied by this group include gadolinium silicide, which has a Curie temperature at about room temperature. Generally the Faraday rotation is proportional to the magnetization below the Curie temperature. These studies indicate that, by proper selection of the combination of elements, both the Curie temperature and the Faraday rotation can be controlled.

Despite these problems with materials, great hope has been stimulated by demonstrations of writing on MnBi thin films. Typical recorded spots were as small as 1 micron in diameter, with the distance between spots ranging from 3 to 10 microns. Hence, the capability of designing films suitable for this scheme of data storage, and the capability of storing data in very small bits, have been demonstrated. Research is continuing to perfect these techniques.

Significant unanswered questions remain. For example, how does one locate a specific bit of micro-stored data? Closely related to this question is the problem of spatial control of the laser beam. A technique is needed to place the beam quickly on a specific bit of data. When one considers data bits of micron sizes, physical movement of the laser or the data-storage thin film seems unrealistic. Beam motion by means of altering the transmission characteristics of solid-state materials is still not sufficiently advanced to suggest answers.

This field of high-priority research will receive even greater emphasis in years to come. The ultimate solutions will probably incorporate principles not yet recognized as relevant to this area, such as the increasingly popular electroacoustic work.(4)

REFERENCES

(1) Mayer, L., "Magnetic Writing with an Electron Beam," *Journal of Applied Physics*, Vol. 29, p. 1454, 1958.
(2) Tchernev, D., "Extremely High Density Magnetic Information Storage," *IEEE Transactions on Magnetics*, March 1968.
(3) Mayer, L., "Curie-Point Writing on Magnetic Films," *Journal of Applied Physics*, Vol. 29, p. 1003, 1958.
(4) Kantak, J. F., "Opcoustic," *OAR Research Review*, Vol. VII, No. 7, July 1968.

** Col Kalisch wrote this article while he was still at AFOSR. He is now at AFCRL.*

IMPROVING THE QUALITY OF WEATHER-SATELLITE PHOTOS

METEOROLOGY LABORATORY, AFCRL

One problem with weather-satellite photos is their poor quality. A lack of contrast results in a gray, washed-out appearance and obscures valuable detail. Robert F. Myers of AFCRL has recently completed a study of weather-satellite picture quality, has identified the factors involved, and has shown how this quality can be enhanced at the receiver with a little effort.

Myers' work is described in the AFCRL report, "Factors Affecting the APT Picture Quality" (AFCRL-68-0517). The "APT" referred to in the title is the Automatic Picture Transmission equipment carried aboard weather satellites launched within the past few years—ESSA II, ESSA VI, and NIMBUS II. The APT satellite equipment is designed to be used with ground-based APT receivers. These receivers are not unduly expensive, costing under $50,000 each, and are commercially available. Several hundred are in operation all over the world, with the Weather Bureau and the Air Weather Service each operating a sizeable number.

Robert F. Myers of AFCRL (right) with Major Alfred C. Molla, Jr., Air Weather Service liaison officer to the National Environmental Satellite Center. Mr. Myers has shown that it is possible to improve the quality of weather-satellite photos through the proper alignment and calibration of the receiving equipment.

Picture quality—or the lack of it—originates in the vidicon camera in the satellite. This camera has inherent limitations. One of these is the fact that the output voltage of the vidicon covers an image brightness range of about 700- to 5,000-foot lamberts, while extremely bright clouds may have luminance values above 10,000. These extremely bright clouds are often of a thick cumulus type—the very ones of maximum importance to the meteorologists. Another picture transmission problem is the fact that each weather satellite has a different camera sensitivity. In any event, there is not much that can be done about transmission quality.

Let's look at the APT recorder where, without equipment redesign or modification, we can do much to improve weather-satellite pictures. Myers points out in his report that poor picture quality is often the result of imprecise calibration and a lack of understanding on the part of the operators of those factors which affect the quality of a picture.

For example, the operator should know that aging of the vidicon in the space environment not only changes the dynamic range of the video signal but also that the loss of sensitivity is more severe at low-brightness levels than at high-brightness areas of the picture. In the recorder itself the gray scale compensation circuits can be used to compensate for vidicon degradation. These compensating changes can be maintained from picture to picture if the recorder itself does not introduce variability into the picture processing.

Another AFCRL investigation has shown that machine temperature has

caused the major variations in the photographic process. All other sources of variability, except the light source itself, were overshadowed by this one effect. To overcome this temperature problem, AFCRL has constructed a temperature-controlled oil bath to keep the machine at an internal temperature of 80 degrees F. Since the temperatures of the photographic paper and chemical developer also affect picture quality, both should be kept at a temperature of 80 to 85 degrees F.

The biggest factor affecting picture quality is one relating to the dynamic range of the transmitted signal. The dynamic range, which establishes the gradations of contrast in the received picture, varies from satellite to satellite. This requires that a special gray scale be formulated for each satellite. Myers has worked out methods for obtaining an optimum gray scale for each satellite, and for updating the gray scale as the aging of the satellite cameras changes its dynamic range. The gray scale is derived from considerations of contrast between water and clouds or between water and land. The report instructs APT operators in the method of obtaining the optimum gray scale for a given satellite, and lists the adjustments that must be made on the equipment to obtain the best picture.

To get satellite weather pictures of uniform high quality from the APT equipment, Myers suggests that operators should institute a program for the daily routine calibration of the equipment.

When additional recorders were recently procured by AFSC's Electronic Systems Division for use in Southeast Asia (SEA) to accommodate the infrared transmission from Nimbus III, many of AFCRL's modifications had been incorporated by the manufacturer into the new machine. These machines are now producing pictures of exceptional quality in SEA.

Mr. Robert F. Myers is a general research physical scientist at the Meteorology Laboratory, AFCRL. He is currently engaged in work in ozone instrumentation and in the development of a system to provide wind and density information from the unattended Doppler radar measurements of meteor trails.

In 1936, Mr. Myers received a Bachelor of Science degree in Chemical Engineering from the Virginia Polytechnic Institute. Later he attended the Aerological Engineering course at the Postgraduate School of the U.S. Naval Academy, and took several courses in mathematics and physics at the University of Tennessee Graduate School.

Prior to coming to AFCRL, Mr. Myers had worked for the Weather Bureau and served as an Aerological Officer on active duty with the U.S. Navy. In 1955, he joined the Geophysics Research Directorate, AFCRC (predecessor of AFCRL), working in the area of meteorological data handling. Later, as Chief of the Meteorological Equipment Branch, he was responsible for the development of meteorological ground equipment for the Air Force. He was assigned to the Meteorology Laboratory as a senior research engineer in 1960.

Mr. Myers is a member of the American Meteorological Society and has a number of publications to his credit.

new radar technique for detecting cloudy-air turbulence

METEOROLOGY LABORATORY, AFCRL

A new technique for detecting severe turbulence in storms and for displaying this turbulence on a radar PPI has been developed and tested by AFCRL. When used at large air terminals, this technique will enable air traffic controllers to guide aircraft around the hazards of severe cloudy-air turbulence during the critical let-down and climb phases of the flight.

The system, called the Plan Shear Indicator (PSI), was developed by Graham M. Armstrong and Ralph J. Donaldson of AFCRL. It uses a Doppler weather radar and a coherent memory filter coupled with an ordinary PPI scope. The coherent memory filter is the key component in the system. Essentially, it is a specialized spectrum analyzer having the capability of producing Doppler spectra at all radar ranges almost simultaneously.

Present operational weather radars can guide pilots around the dense centers of stormy cloud systems where turbulence is often severe. But, just as often, the areas of most severe turbulence are found outside the dense core of a convective cell. The PPI display from a conventional weather radar tells us nothing about internal wind velocities. We see only the large silhouettes of storm systems. More sophisticated Doppler systems can detect wind fields within storms; but they sacrifice real-time display capability because of excessive data-processing time.

On AFCRL's PSI display we see the same cloud system; but instead of the solid silhouette, we see that the storm is represented by discrete lines—like a TV picture. The lines are arranged in concentric arcs out from the radar location, and represent range-gated intervals of about a half-mile separation. But they also represent wind-velocity information. In other words, range and velocity information share the same coordinate on the PSI display. Thus, the line is displaced by a given distance depending on the wind velocity.

Now, if we assume radial wind components of a uniform velocity throughout the cloud system—or no motion at all, as in the case of fixed ground targets—the lines forming the PPI picture of the storm system would all be parallel and uniformly spaced. However, a sharp change in wind direction or velocity will cause a distortion of the lines at the range interval where the change occurs. When severe localized turbulence occurs, the lines at that location will be broadened.

The alterations in the lines forming the picture of the storm are generated by the spectral analysis of the detected radar signal. The spectral data are used to position a particular range arc on the PPI. If the winds are moving away from the radar at a given velocity, the line will be displaced inward toward the radar with an increment depending on its velocity. If the wind is moving toward the radar, the line is displaced outward. Severe localized

turbulence results in spectral broadening (because the radar cannot resolve details in this turbulence) and this tends to thicken the line.

Wind shear, turbulence, sinks, and vortices can all be interpreted by the pattern depicted by the lines. A wind-shift line of the type which might accompany a frontal passage is seen as a sharp displacement cutting across several lines. A vortex is seen as a wave-like structure in several parallel lines. This structure is produced as the winds move toward the radar at one edge of the vortex and away from the radar at the opposite edge.

Donaldson and Armstrong have tested the system against several local storms in the vicinity of AFCRL's Weather Radar Site at Sudbury, Mass. with excellent results. The Sudbury test radar operates at 5.4-centimeter wavelength, and has a range of 88 miles. The PSI system may also be adapted for airborne use, although problems of economy, weight, and space must still be solved.

Mr. Ralph J. Donaldson is a research physicist at the Weather Radar Branch of the Meteorology Laboratory, AFCRL. He has been engaged in weather radar research at AFCRL since 1953. In this work, he has studied thunderstorms and squall-line systems, developed new techniques for the remote identification of severe thunderstorms by radar, and investigated the structure and air flow of storms that produce tornadoes. Currently, he is studying thunderstorms by the use of Doppler radar.

After completing Army courses in Meteorology at Chanute Field in 1944, and in Electronics and Radar at Harvard and M.I.T. in 1945, he was graduated from Wooster College, Ohio, with a B.A. in Physics in 1947. His graduate work was taken at Harvard, where he received a Master of Science degree in Applied Physics in 1949.

During World War II, Mr. Donaldson was a weather forecaster and radar weather officer in the Air Weather Service. He came to what is now AFCRL in 1949 as a research assistant in ionospheric physical studies. He is a member of the American Meteorological Society, and RESA.

Mr. Graham M. Armstrong is an electronic engineer at the Weather Radar Branch, Meteorology Laboratory, AFCRL where, since 1964, he has been concerned with the development of new techniques for probing the atmosphere with pulse Doppler radar and with the analysis of experimental data on thunderstorms obtained from Doppler radar.

After receiving an Associate Degree in Electronic Engineering with honors from Northeastern University in 1959, Mr. Armstrong received a B.B.A. from the same University, in 1961, with a major in Engineering and Management. Since 1961 he has taken various mathematical and engineering courses at the Northeastern University Graduate School.

From 1953 to 1964, Mr. Armstrong was employed as an electronic development technician with the Weather Radar Branch.

Ralph J. Donaldson (left) and Graham M. Armstrong are two of the nation's leading investigators of Doppler weather radar. Their radar techniques for detecting areas of turbulence in cloudy air represent a sizeable quantum jump forward in weather radar methods of procedure.

GPO 881-401

TO OUR READERS

Requests for further information should be directed to the individual or laboratory of origin (except for those from Latin America).

Addresses are as follows:

AIR FORCE CAMBRIDGE RESEARCH LABORATORIES
Attn: CRI
Laurence G. Hanscom Field, Bedford, Massachusetts 01730

AEROSPACE RESEARCH LABORATORIES
Attn: ARI
Wright-Patterson Air Force Base, Ohio 45433

AIR FORCE OFFICE OF SCIENTIFIC RESEARCH
Attn: SRGC
1400 Wilson Blvd, Arlington, Va. 22209

THE FRANK J. SEILER RESEARCH LABORATORY
USAF Academy, Colorado 80840

DET.8(ORA)OAR
Attn: RRR
Holloman Air Force Base, New Mexico 88330

Requests for further information from institutions and individuals in Latin America should be addressed to:

DET.7 (LAOAR)OAR
U.S. Embassy-Rio
APO New York 09676

Detailed documentary reports may be obtained from:

CLEARINGHOUSE
U.S. Department of Commerce, Springfield, Virginia 22151

DEFENSE DOCUMENTATION CENTER*
Cameron Station, Alexandria, Virginia 22314

*Qualified requesters

OAR (RRYC)
1400 WILSON BLVD
ARLINGTON, VA 22209

UNITED STATES AIR FORCE
OFFICIAL BUSINESS

POSTAGE AND FEES PAID
DEPARTMENT OF THE AIR FORCE

★ AIR FORCE CAMBRIDGE RESEARCH LABORATORIES
★ AIR FORCE OFFICE OF SCIENTIFIC RESEARCH
★ AEROSPACE RESEARCH LABORATORIES
★ OFFICE OF RESEARCH ANALYSES
★ LATIN AMERICAN OFFICE OF AEROSPACE RESEARCH
★ THE FRANK J. SEILER RESEARCH LABORATORY
★ EUROPEAN OFFICE OF AEROSPACE RESEARCH